

FINAL PUBLISHABLE JRP REPORT

JRP-Contract number	IND16	
JRP short name	Ultrafast	
JRP full title	Metrology for ultrafast electronics and high-speed communications	
Version numbers of latest contracted Annex Ia and Annex Ib against which the assessment will be made	Annex Ia:	V1.0
	Annex Ib:	V1.0
Period covered (dates)	From 01 July 2011	From 30 June 2014
JRP-Coordinator		
Name, title, organisation	Dr. Mark Bieler, Physikalisch-Technische Bundesanstalt (PTB)	
Tel:	+49-531-592-2540	
Email:	mark.bieler@ptb.de	
JRP website address	www.ptb.de/emrp/ultrafast.html	
Other JRP-Partners	CMI, Czech Republic INTA, Spain LNE, France MIKES, Finland NPL, UK VSL, Netherlands AGILENT, UK	
REG1-Researcher (associated Home Organisation):	Dr. Sajjad Ahmed NIBNV, Belgium	Start date: 01 June 2013 Duration: 12 months
REG2-Researcher (associated Home Organisation):	Dr. Gennaro Gentile TU Delft, Netherlands	Start date: 01 September 2012 Duration: 12 months

Report Status: PU Public



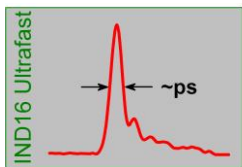


TABLE OF CONTENTS

1 Executive Summary 3

2 Project context, rationale and objectives 4

 2.1 Primary waveform standards 4

 2.2 Uncertainty propagation between time- and frequency domain for long data sets 5

 2.3 Novel communication links at high carrier frequencies 5

 2.4 Traceability of digital signals 6

3 Research results 7

 3.1 Development of laser-based techniques for the measurement of pulsed and cw high-frequency signals 7

 3.2 Provision of a software tool for uncertainty propagation that can be applied to long data sets and is available free of charge 11

 3.3 Investigation of antenna and channel properties in the mm- and sub-mm wave range 15

 3.4 Establish methods for traceable calibration of vector signal generators and analysers and develop tools for a better understanding of the measurement uncertainty of digital signals 21

4 Actual and potential impact 26

 4.1 Societal benefit 26

 4.2 Strategic approach to impact within this project 26

 4.3 Dissemination activities 27

 4.4 High-profile events and awards 27

 4.5 Workshops 27

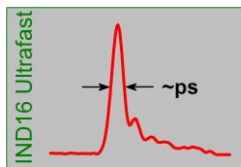
 4.6 Exploitation and uptake 28

 4.7 Contribution to longer-term impacts 29

 4.8 Effective cooperation 29

5 Website address and contact details 29

6 List of publications (chronological order) 30



1 Executive Summary

Introduction

This project has significantly contributed to the traceable characterisation of ultrafast and high-frequency electronic instrumentation. This is a prerequisite for new and enhanced developments of high-speed communications and remote sensing applications.

The Problem

The use of higher frequency bands for mobile data transmission as well as higher electronic processing speeds requires that suitable high-frequency measurements can be made in the design, production and implementation of ultrafast systems. For the measurement of high-frequency or ultrafast signals the frequency response of the measurement instrumentation needs to be known since it affects the measured signal considerably. This may have severe influences on, e.g., the result of pass/fail tests employed in production environments or new design considerations. It is thus of great importance to know to what extent high frequency signals are altered when being measured. Moreover, measurements of ultrafast systems produce extremely datasets for which there was no simple and easy to apply measurement uncertainty calculation algorithms existed. As the bandwidth and complexity of modern communication systems continually grows, the need for a traceable characterisation of measurement equipment is more urgent than it has ever been.

The Solution

To enable accurate measurement of ultrafast or high frequency signals the project developed new measurement techniques and enhanced existing measurement techniques based on femtosecond lasers. These techniques have a larger bandwidth and are less invasive than conventional all-electronic measurement techniques. Such developments will be important for manufacturers and users of high-speed and high frequency measurement instrumentation.

Using such instrumentation for measurements over long time windows often yields time traces with more than 10,000 data points. In order to perform uncertainty calculations with such long traces, the project developed a compression algorithm, which has much less storage requirements than existing algorithms. The software tool is available free of charge and available to calibration labs, NMIs, and industry.

Future communication systems will be very different compared to today's systems in terms of much higher bandwidth located at considerably higher frequencies and smart and flexible system architectures. For such enhanced communication schemes, the project characterised antennas and propagation channels and studied diffraction and scattering at frequencies between 50 GHz and 325 GHz. Moreover, transmission measurements of digital signals at 300 GHz with different digital modulation schemes were performed to investigate the feasibility of implementing such frequencies in future communication systems.

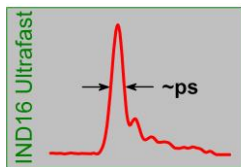
Finally, the exact measurement of digital signals was required to support present and future developments in ultrafast communications. The project developed a universal method for calibration of digital signal instrumentation and the accuracy of a commercial software package for the analysis of digital signals was studied. A simple software tool for the demodulation of basic digitally modulated signals was created; the software is available free of charge.

Impact

The project adopted a structured approach to impact generation so that it could reach a wide cross-section of the technical community. This included conference and journal papers, summarising the research; contributions to standards bodies, to support longer term industrial impact; user guides and trade journal publications that will reach a larger number of scientists and engineers and finally freely available software so that the results could be evaluated.

Overall, the project members gave 53 presentations, including two plenary talks, at national and international conferences; 9 peer-reviewed journal papers and 3 trade journal papers were submitted and 16 training activities were undertaken. Workshops were organised at the European microwave conference EuMC in 2012 and 2013. EuMC is the main European conference in this technical area.

IND16 Ultrafast



Seven user guides have been written, which will be disseminated to users in industry, calibration laboratories and National Metrology Institutes (NMI). Most likely new calibration services will be established at the NMI level. This includes ultrafast waveform measurements, but also measurements of digital signals. Two stakeholders have expressed their interest in the possibility of offering calibration services for vector signal analysers and generators based on the technique developed during this project. At present exact future developments are confidential.

There have been five uptakes of the software packages developed in this project and the application for Subsequent research projects suggests that impact can be also achieved in other fields, such as spectroscopy at terahertz frequencies.

Links with two international and three national standards committees have been established. Members of the project contributed to a new standard on the calculation of waveform parameter uncertainties (IEC TC 85, WG22). This new standard is expected to be made public in 2015 and is applicable to all industries that generate, transmit, detect, receive, measure and/or analyse step- and impulse-like waveforms.

The improved methods for characterisation of high-frequency measurement instrumentation resulting from this project directly increase the level of confidence in their design and fabrication processes because various quantities can be measured with smaller uncertainties. This is the prerequisite for better designs of high-frequency communication and remote-sensing products, such as ultrafast sampling oscilloscopes and vector signal analysers and generators. Society will benefit from these new developments as new communication techniques will help to ensure availability of information at any place and at any time.

2 Project context, rationale and objectives

The steady increase of the speed and bandwidth of new communication systems and remote sensing applications continuously improves the quality of life of many people worldwide. As proposed in the International Technology Roadmap for Semiconductors this development is expected to continue undamped over the next decade. Yet this development creates measurement challenges – the performance of ultrafast electronics and communications devices and systems needs to be measured and characterised by measuring instrumentation that can operate at such high speeds and high frequencies – but for which the underlying metrology was not in place. The main aim of this research project was to offer solutions to these challenges and to support the European industry to play a global lead role in ultrafast electronics and high-speed communications for both present as well as next-generation technology. For this purpose, we identified four technical areas which build upon each other:

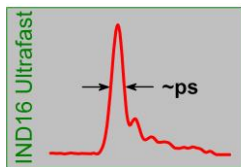
2.1 Primary waveform standards

Ultrafast sampling oscilloscopes and ultrafast pulse generators mark the frontier of today's commercially available high-frequency instrumentation. However, when using these instruments one often ignores that their frequency response is not flat, leading to incorrect measurements. This particularly causes problems when the bandwidth of the device under test approaches the bandwidth of the measurement device. To determine the time response of ultrafast sampling oscilloscopes or pulse generators, it is necessary to employ even faster measurement techniques. Optoelectronic techniques, in combination with femtosecond lasers, are well suited for this purpose.

At the start of the project three NMIs (PTB and NPL in Europe and NIST in the USA) had established optoelectronic measurement techniques for ultrafast electrical signals on coplanar and coaxial lines. Several years before the start of the project a single parameter characterisation, i.e., the measurement of the rise time of the step response, had been extended to waveform metrology where the uncertainty of each time (or frequency) step could be specified. Yet, further developments were required to enhance the existing technologies such that full waveform calibration of a passive device like a sampling oscilloscope is possible.

In addition to the characterisation of a passive device, laser-based measurement techniques also enable characterisation of the amplitude and phase of active high-frequency devices. Electrical pulse generators are important devices since they can act as cheap transfer standards used to characterise the phase response of signal measurement instrumentation, such as oscilloscopes, vector signal analysers, and large signal network analysers. Before the project, a waveform calibration of such a device has only been performed using a

IND16 Ultrafast



calibrated sampling oscilloscope. No attempts for a full waveform characterisation of a pulse generator using laser-based electro-optic sampling, which might yield a considerably reduced uncertainty, had been reported.

A similar situation existed for the measurement of amplitude and phase of continuous wave (cw) sources with an emission frequency of several 10 GHz or larger as needed for the specification of antenna patterns. Purely electrical detection systems constitute the state-of-the-art technology. Yet in order to avoid phase errors, which are prominent especially at higher frequencies, a laser-based optical read-out of the amplitude and phase information offered the potential to greatly improve the accuracy of the measurement of the antenna near-field pattern.

To address the deficiencies the first objective of this research project was the **“Development of laser-based techniques for the measurement of pulsed and cw high-frequency signals”**.

2.2 Uncertainty propagation between time- and frequency domain for long data sets

Measured time-domain waveforms, with even point spacing, can easily be transferred into the frequency domain using standard Fast Fourier Transform (FFT) routines. However, the uncertainty propagation from the time domain into the frequency domain is not trivial, since the simple uncertainty propagation techniques according to the Guide for the Expression of Uncertainty in Measurement (GUM) cannot be applied to waveforms. This also holds for frequency-domain deconvolution techniques which are ill-posed problems if the noise level is strongly increased by a division in the frequency domain.

The covariance matrix in combination with a Fourier transform is a promising technique that allows uncertainty propagation between the time and frequency domain as demonstrated by NIST¹. A key element driving the covariance approach developed at NIST was the link between time-based electro-optic measurements and frequency-based measurements using an Automatic Network Analyser (ANA). Obtaining correlated errors across the frequency spectrum, this mathematical tool is an essential part of the NIST calibration process. The size of the covariance matrix grows proportional to the square (n^2), of the number of data points (n) in the time domain waveform. For traditional sampling oscilloscopes (about 4,000 points), this is within the bounds of readily available computer systems. However, increasing the measurement epoch to 100,000 points as possible with sampling oscilloscopes and even beyond this value as possible with real-time oscilloscopes will cause severe problems. Similarly, large data sets can be obtained with frequency-domain instrumentation. For example, a comb generator similar to the unit tested by REG1 could have a comb frequency spacing of 100 kHz and an upper limit of 67 GHz, set by the geometry of connector (1.85 mm). This would generate a $2.25 \cdot 10^{11}$ point covariance matrix. Additionally, it would require at least 335,000 measurements to form a full-rank covariance matrix. This is impractical for both processing and for storage. Prior to the project, calculations employing such big matrices could not be accomplished using standard computer systems and such algorithms would be impractical for embedded systems. The objective of this work in the project was to provide a practical algorithm to overcome these difficulties.

Uncertainty propagation between the time and frequency domain can also be realised using Monte-Carlo simulations. Recently the Supplement 1 to the GUM was published detailing uncertainty propagation with such simulations. This approach is used at PTB for the primary standard mentioned in Section 2.1 and also allows one to obtain correlated errors in the frequency and time domain. Yet, a multivariate random number generation as used for Monte-Carlo simulations is a time- and memory-consuming task. When using Monte-Carlo simulations on a standard computer system for long (>10,000 points) data sets, it is even necessary to save intermediate results on the hard-disk. Thus, Monte-Carlo simulations can certainly not be used as an easy and quick tool for uncertainty propagation between the time and frequency domain.

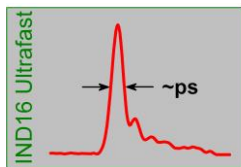
Therefore the second objective of this research project was the **“Provision of a software tool for uncertainty propagation that can be applied to long data sets and is available free of charge”**. The rationale for this objective is to maximise impact by minimizing the effort required for a potential end-user to evaluate the algorithms.

2.3 Novel communication links at high carrier frequencies

The increased need for unoccupied and unregulated bandwidth for future wireless short-range communication systems as well as for new remote sensing applications will require the increase of operation frequencies in

¹ D. F. Williams et al., IEEE Trans Microw. Theory Tech. vol. 54, no. 1, pp. 481 – 491, Jan 2006.

IND16 Ultrafast



the millimetre wave range and the more efficient use of bandwidth. Current wireless local area network (WLAN) standards offer data rates up to 54 Mbps at frequencies of 2.4 GHz, 5.2 GHz and 5.8 GHz while more recent developments in the field of ultra-wide-band (UWB) communication reach 500 Mbps using the spectral range between 3.1 GHz and 10.6 GHz. In the future, the millimetre wave band around 60 GHz with unlicensed 5 GHz bandwidth in Europe and 7 GHz bandwidth in the US is also considered as a potential host for UWB communication with even higher data rates. Channel sounding as required for reliable channel modelling and system design at 60 GHz is the subject of ongoing research. Together with car-radar at 77 GHz these applications mark the frontier for commercially widespread technology. While the frequencies above that have long been used in fundamental research, new compact sources and detectors are now appearing on the market that enable practical applications, including sensing and communications. Recently, indoor communications at 300 GHz has been proposed and hardware solutions for transmission experiments and channel measurements have been shown at this frequency.

Communication links at frequencies beyond those in use for communication applications today will have to rely on directed line-of-sight or non-line-of-sight transmission using high gain antennas. Such antennas will have to be phased arrays that use innovative system concepts (e.g. MIMO – multiple input multiple output). The improvement of such antennas requires reliable measurements that take into account these system concepts but which are rarely available at present. Communication system design and improvement have to rely on the accurate determination of signal transmission properties. A quantitative evaluation of the influence of the transmission channel and hardware used for up- and down-conversion on the signal properties does not exist. However, knowledge of this influence is crucial for the proper choice of suitable modulation techniques in future high-speed communication systems.

To address the current deficiencies the third objective of this research project is the **“Investigation of antenna and channel properties in the mm- and sub-mm wave range”**.

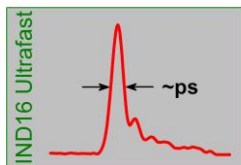
2.4 Traceability of digital signals

Currently the frequency spectrum allocation is lacking sufficient free and unregulated bandwidth to host advanced new services with increasingly high data rates. Wireless communication systems use a variety of advanced modulation and coding techniques in order to increase the data rates and to make the links more reliable and robust. To guarantee an interoperability of wireless systems, specification standard bodies such as 3GPP (3rd generation partnership project) release regulation documents with recommendations on how to properly measure and design various wireless systems' aspects.

The traceability to measurement standards is well established for average parameters such as RF power. However, traceability is difficult to achieve for dynamic measurements such as modulation envelope or error parameters of modulated signals. This especially holds for the error vector magnitude, EVM, which is one of the key parameters used to define the performance of wireless communication equipment and circuits. Usually these parameters are estimated with regard to baseband measurements. However, manufacturers of measurement instruments use slightly different methods to calibrate their own instruments. Moreover, the calibration usually forms a closed loop, e.g., for the calibration of a vector signal generator, one needs a calibrated vector signal analyser and vice versa. These methods are clearly not traceable to standards of a higher precision, which causes problems with design and verification of interoperable wireless devices for different markets. To establish traceability NPL proposed a strategy for a waveform metrology technique which is based on oscilloscopes and forms an unbroken chain between the optoelectronic primary standard (see section 2.1) and the modulated RF waveform.

In addition to the frequency (amplitude and phase) response of vector signal analysers and generators an unsatisfactory situation also existed for the uncertainty propagation of digital signals, e.g. uncertainty of the measured EVM. Although proprietary software is currently available for use with communications instrumentation, this software does not provide any information about the measurement uncertainty. Yet, specification of the uncertainty and, thus, the traceability is a key requirement of ISO 17025 (“General requirements for the competence of testing and calibration laboratories”) for calibration laboratories and instrument manufacturers.

To address the current deficiencies the fourth objective of this research project is to **“Establish methods for traceable calibration of vector signal generators and analysers and develop tools for a better understanding of the measurement uncertainty of digital signals”**.



So the four objectives of this project were:

1. To develop laser-based techniques for the measurement of pulsed and cw high-frequency signals.
2. To provide a software tool for uncertainty propagation that could be applied to large data sets and would be available free of charge.
3. To investigate antenna and channel properties in the mm- and sub-mm wave range; and
4. To establish methods for traceable calibration of vector signal generators and analysers and develop tools for a better understanding of the measurement uncertainty of digital signals.

3 Research results

In this section the research results of the four scientific objectives above will be described.

3.1 Development of laser-based techniques for the measurement of pulsed and cw high-frequency signals

The aim of this work was to establish traceability of high-speed and high-frequency measurement instrumentation. This has been accomplished using optoelectronic measurement techniques based on femtosecond lasers. The time (and frequency) axis for such techniques is traceable to the SI. The work addressed immediate industry needs as the resulting primary standards were placed at the top of a calibration chain and additionally laid the basis for metrology of future high-speed and high-frequency devices.

3.1.1: Primary standard for waveform metrology

In this subsection the development of a laser-based voltage pulse standard is described. The voltage pulse standard was realised on a coplanar waveguide (CPW) and had frequency components larger than 500 GHz and 500 MHz frequency spacing, i.e., measurements were performed over a time window of 2 ns. The ultrashort voltage pulses were generated by focusing a laser beam (~350 fs pulse width, ~800 nm centre wavelength, 76 MHz repetition rate) onto a biased photoconductive gap, which was integrated into a 4-mm long CPW. The CPW was evaporated onto low-temperature-grown GaAs (carrier life time ~1 ps) and had a characteristic impedance of 50 Ω at low frequencies. A second laser beam (~100 fs pulse width, ~1600 nm center wavelength, 76 MHz repetition rate), which was synchronised to the first laser beam was used to measure the electric field of the voltage pulses by employing the electro-optic (EO) effect of the GaAs substrate and a typical electro-optic detection set-up. By changing the time-delay between the two laser pulses the shape of the voltage pulse was obtained.

In order to terminate the CPW and to be able to transfer the voltage pulses to coaxial 1.85-mm structures, a microwave probe (MWP) was attached to the end of the CPW. Additionally, a 40-cm long coaxial semi-rigid cable terminated with a load was connected to the coaxial end of the MWP. Although all components had a characteristic impedance of 50 Ω , transmission line discontinuities were generated at each connection and small reflections occurred, especially at higher frequencies. This is demonstrated in Figure 1(a), where the shape of a voltage pulse measured after propagating 2 mm on the 4-mm long CPW is shown over a measurement epoch of 2 ns. As visualised by the upper inset, the voltage pulse has frequency components exceeding 500 GHz. The lower inset magnifies a time epoch of approximately 100 ps which displays a significant voltage signal even several 100 ps after the main voltage pulse. From this single measurement it was impossible to distinguish the forward and backward propagating signals from each other, which is an essential prerequisite for the realisation of a voltage pulse standard.

For the distinction between forward and backward propagating signals we employed a model which was based on the measurement of two voltage pulses $v_1(t)$ and $v_2(t)$ at different positions on the CPW. This model, as detailed in [10], yielded the complex reflection coefficient Γ at the measurement plane on the CPW. The result for Γ obtained with this model is plotted in Figure 1(b), where the impulse response of Γ is shown. This time-domain representation allowed for an easy interpretation of the results. The largest reflection occurred from the position where the MWP is attached to the CPW. Moreover, there were subsequent reflections which occurred within the MWP and from the connection between the coaxial end of the MWP and the long cable. No reflections could be detected afterwards (within the measured time window of 2 ns).

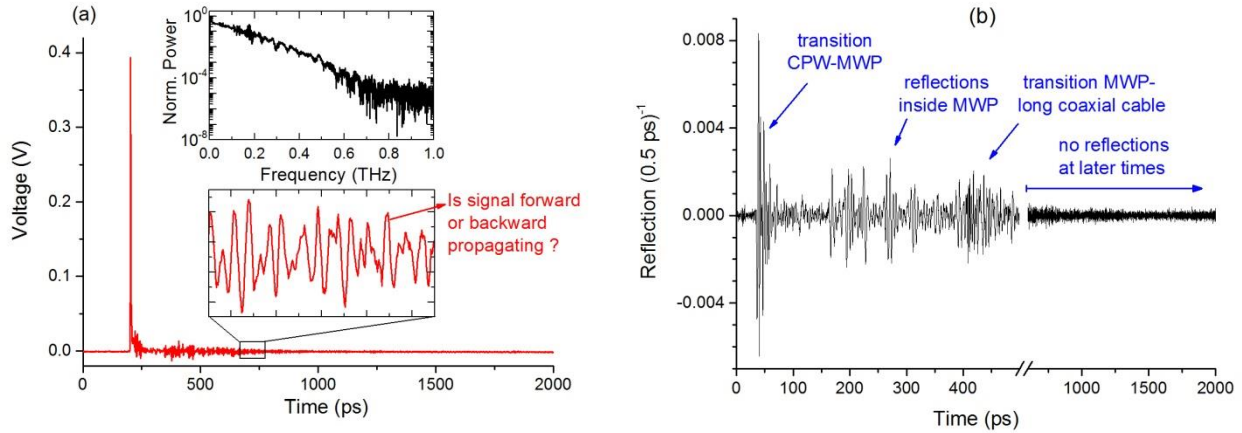
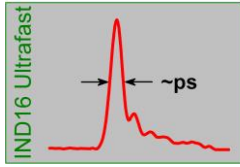


Figure 1: (a) Measurement of a voltage pulse over an epoch of 2 ns after propagating 2 mm on a 4-mm long CPW. The upper insets show the frequency spectrum of the voltage pulse while the lower inset magnifies the signal of the voltage pulse around 700 ps. (b) Impulse response of the reflection coefficient Γ . One can clearly observe several transmission line discontinuities.

3.1.2: Full waveform characterisation of ultrafast sampling oscilloscopes

The development of the voltage pulse standard (discussed in Section 3.1.1) was employed for the calibration of the time response of an ultrafast sampling oscilloscope (LeCroy SE70 with nominal bandwidth of 70 GHz). The main equation for the transfer function of the oscilloscope H_{osc} is as follows:

$$H_{osc} = \frac{V_{osc}\left(\frac{t}{\gamma}\right)H_{EOS}}{V_{fw,CPW}S_{12,MWP}e^{-2(\pi\sigma_j f/\gamma)^2}} \quad (1)$$

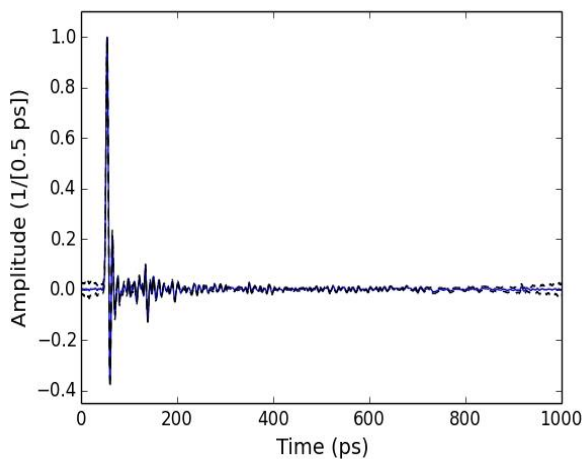


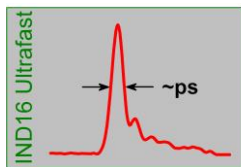
Figure 2: Impulse response of the sampling head plotted over different time windows. The blue line shows the mean of 1000 MC realisations, while the black lines denote the 95% confidence interval. This mode showed basically no systematic time base distortion. Spline interpolation was used to obtain an evenly spaced time step identical to the one of the laser-based measurements.

The oscilloscope jitter σ_j was measured in the statistics mode of the oscilloscope (without averaging). The time base correction factor γ is defined as $t_{real} = \gamma t_{osci}$ with t_{osci} and t_{real} being the oscilloscope's time base and the corrected time base of the oscilloscope, respectively. In order to determine γ the features resulting from

Here, V_{osc} is the Fourier transform of the measured oscilloscope trace, γ is the time-base correction factor of the oscilloscope, σ_j is the oscilloscope jitter, and H_{EOS} denotes the transfer function of the EO sampling technique as described in [10]. The waveform obtained from the voltage pulse standard is denoted by $V_{fw,CPW}$ and $S_{12,MWP}$ denotes the transfer function from the measurement plane on the CPW to the coaxial connector of the oscilloscope head.

The quantities $V_{fw,CPW}$ and $S_{12,MWP}$ were obtained from laser-based measurements; and it was found that the uncertainty (especially of $S_{12,MWP}$) of the first frequency points was very large. Thus measurements performed with the current setup over an epoch of more than 1 ns did not yield additional information.

The oscilloscope trace v_{osc} was measured in the



reflections in $v_{fw,CPW}$ and v_{osc} were compared. Since such features must not change the time response of the sampling head, γ could be determined accordingly to 1.0008.

The resulting estimate of the impulse response h_{osc} which is the inverse Fourier transformation of H_{osc} is depicted in Figure 2, together with the pointwise 95 % coverage intervals. A FWHM of the impulse response of 5.1 ps with a 95 % coverage interval ranging from 4.9 ps to 5.3 ps was obtained.

3.1.3: Characterisation of electric pulse generators

As an alternative to a synchronised laser-based measurement setup, as used in Sections 3.1.1 and 3.1.2, the technique of asynchronous optical sampling (ASOPS) was already introduced several years ago. Here, two pulsed laser sources with a slightly detuned repetition rate allow for a high-speed sampling process of the optically generated signal. However, the aforementioned studies focused on the analysis of purely optically generated signals. Different considerations had to be taken into account for the analysis of purely electrically generated signals. In the work described in this subsection ASOPS for the characterisation of an all-electronic pulse generator was investigated. These devices are important tools as they serve, e.g., as harmonic phase references for the calibration of modulated RF and microwave signals.

To demonstrate the usability of the ASOPS technique for the characterisation of an electronic signal, a pulse generator with voltage amplitude of approximately -370 mV and a nominal bandwidth of 40 GHz was utilised. This pulse generator was loaned from one of our Researcher Excellence Grant partners. The pulse (or comb) generator can be operated in different modes, including a divider mode, a pseudo-random-binary-sequence (PRBS) mode, and a combined divider-PRBS mode. All measurements were performed in divider mode. Here, the pulse repetition frequency was determined by a clock signal provided by a local oscillator. Via software control, the clock rate was further divided by integer values $i = 1, 2, 4, 8, \dots$ to allow for a wide range of pulse repetition rates. The driving frequency $f_{LO1} = 2.432003697$ GHz and a divider value of $i = 32$ resulted in a pulse repetition frequency of $f_i = f_{LO1}/i = 76000115.53125$ Hz. The output signal of the pulse generator was transferred to a coplanar waveguide (CPW) using a standard microwave probe. The CPW consisted of a 25 μm broad signal stripe separated by 15 μm from two 100 μm broad ground stripes and had a length of 4 mm. The structure was evaporated onto a 500- μm thick GaAs substrate. The characteristic impedance of the CPW was close to 50 Ω . The CPW was terminated by use of a second MWP, which was connected to a 50 Ω load using a 30-cm long semi-rigid cable. By this, reflections of the voltage pulse were minimised. To probe the voltage pulses travelling on the CPW, the EO effect of the GaAs substrate was employed as described in Section 3.1.1.

In Figure 3, the full waveform of the pulse generator over the full period of 13.16 ns obtained from 7000 consecutive measurements over 2 s with a total measurement time of approximately 4 h is shown. Together with the mean value, the standard uncertainty of the 7000 waveforms is plotted. For the construction of the time-domain traces, an evaluation of 7000 times $25 \cdot 10^6$ sample points was necessary. A signal-to-noise ratio (SNR) of the mean waveform of approximately 3200 was obtained; the spectral power of the voltage pulse, touched the noise level at approximately 80 GHz (see inset of Figure 3). The time-domain waveform showed small signals lasting up to 2 ns after the pulse maximum. Since the transfer function of our detection technique was essentially flat in the corresponding frequency range [10], these signals were real and mainly resulted from transmission line discontinuities. The mean of the FWHM of the individual time traces was 20.5 ps, with an expanded ($k=2$, 95 % coverage interval) uncertainty of 1.0 ps.

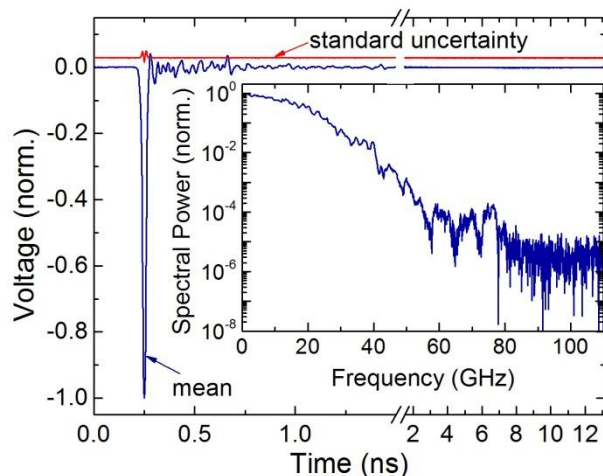
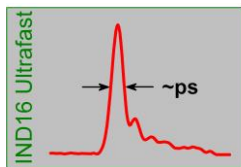


Figure 3: (a) 13.16-ns long waveform of the electrical pulse generator output, acquired using ASOPS. 7000 consecutive measurements over 2 s each have been averaged to reach a signal-to-noise level of the time-domain waveform of about 3200. In the inset, the spectral power of the pulse is shown. With a dynamic range of 50 dB, frequency components up to 80 GHz are detected.



In conclusion, the studies [29] showed that an accurate time trace of the voltage pulses could be constructed from a large number of multiple measurements, which had several advantages. (i) This technique works for the case of limited synchronisation ability between the electrical and optical part of the measurement system, in which synchronised optical sampling is not possible. (ii) Arbitrary time-resolutions can be achieved due to the use of a software-based data analysis scheme. (iii) A detailed uncertainty analysis of the obtained waveform is allowed by the construction of a covariance matrix with full or at least very high rank.

3.1.4 Laser-based coherent electric field measurements in the (sub-) mm-wave region

Recent progress in the development of applications operating in the THz frequency range, e.g., spectroscopy, imaging, and communication technology, required a traceable metrology for the key parameters “frequency”, “phase” and “amplitude”. The main goal of the work described in this subsection was to study whether laser-based techniques could be used for measurements of amplitude and phase of high-frequency antennas. The measurement principle was based on the mixing process between the m -th line of a downconverted (rectified) optical frequency comb and the emission of an antenna under test (AUT) with a frequency f_{THz} . The optical comb was generated by an unstabilised Ti:Sa femtosecond laser with a centre wavelength of 800 nm, a pulse duration of 100 fs and a repetition rate $f_{\text{rep}} \sim 76$ MHz. The downconversion and mixing process could be performed in two ways; and either a photoconductive switch (PCS) fabricated on low-temperature grown GaAs or electro-optic sampling (EOS), employing a 0.5-mm thick GaP crystal was used. Either method was applicable in a wide frequency range from DC up to several THz, limited by the carrier dynamics in the PCS and by the transfer function of the EOS, respectively. In both methods, a beating signal with a frequency of $f_b = |m f_{\text{rep}} - f_{\text{THz}}|$ was generated, which was located between DC and half of the repetition rate. This signal could be easily recorded using standard electronics. In this case a two-channel analogue-to-digital converter (ADC, 10 MHz sample rate and 0.1 s measurement interval) was utilised.

Two different beating signals were sampled in parallel by the two-channel ADC using two separate detection setups. In the first detection setup the AUT was placed. For the data shown in this summary, a frequency multiplier chain (multiplication factor $m=6$) with an output frequency f_{THz} of ~ 100 GHz was employed, but the technique could also be applied to much higher frequencies of several THz. Both detection methods, EOS and PCS, have been employed for the measurement of the amplitude and phase characteristics of the AUT.

In the second detection setup, the beating signal from an antenna whose frequency was harmonically related to the one of the AUT was measured. This was accomplished by using a common signal generator for both antennas. In this work, a frequency multiplier chain with a multiplication factor of $n=2$ was used. The beating signal from this reference antenna was important due to three reasons: (i) it served as phase reference for measurements of the relative phase of the AUT; (ii) it was needed for precision frequency measurements to compensate for repetition rate fluctuations of the femtosecond laser [11]; and (iii) it also allowed compensation for power fluctuations of the femtosecond laser yielding better amplitude measurements.

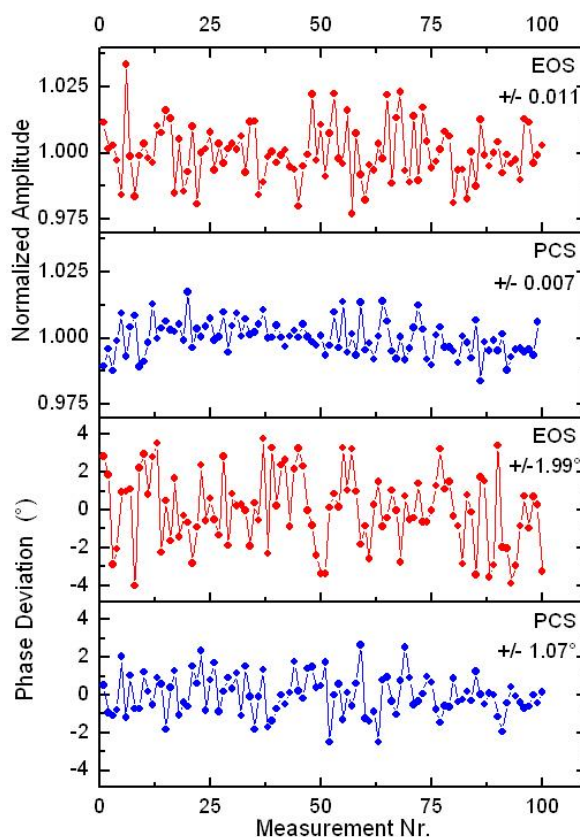
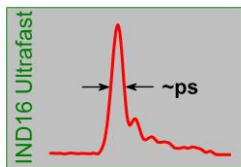


Figure 4: Amplitude (upper two graphs) and phase (lower two graphs) values obtained from 100 consecutive measurements at a fixed AUT position using EOS and PCS detection techniques. The values in the upper right-hand-side corner denote the experimental standard deviation of the 100 measurements.



To evaluate the measurement accuracy of the experimental setup with respect to amplitude and phase, 100 consecutive, 0.1-s long measurements were taken and analysed. As can be seen in Figure 4, different results for the EOS- and PCS-based detection methods were obtained. EOS yielded a standard deviation for a single measurement (standard deviation of the mean) of the relative amplitude of 1 % (0.1 %), whereas the PCS-based method reached a value of 0.7 % (0.07 %). For the phase measurements, the standard deviation of a single measurement (standard deviation of the mean) was 2.0° (0.2°) and 1.1° (0.11°) for EOS and PCS, respectively. While the uncertainty for PCS measurements was slightly lower as compared to EOS measurements, it was believed that this difference was not significant as it depended on many parameters (quality and type of the electro-optic material, carrier lifetime and mobility of LT GaAs, and photodiodes and amplifiers used in the detection process). Thus, it is safe to state that - at least for the experimental conditions of this study - EOS and PCS provided similar signal-to-noise ratios for amplitude and phase measurements.

In conclusion, an experimental setup [11,17] has been introduced showing that THz frequency combs generated from unstabilised femtosecond lasers are well suited for the measurement of amplitude and phase of high-frequency antennas. It should be noted that in additional experiments the setup has been enhanced to allow for spatially resolved and even quantitative measurements [27].

3.2 Provision of a software tool for uncertainty propagation that can be applied to long data sets and is available free of charge

The aim of this work was the provision of a software tool for uncertainty propagation between time and frequency domain that could be applied to large data sets and would be available free of charge. This would allow NMIs and industry to disseminate and use waveform results with uncertainties in a compact format.

NIST had already developed a covariance matrix approach that propagated uncertainties between the time and frequency domains² to underpin their EOS system. The difficulty with this method, for industrial applications, was that the data storage increased with the square of the number of data points and would limit its usefulness for applications such as communications, where the record length is larger than 10,000 points. A key objective was to develop an algorithm that grew more slowly than the square of the number of points, while retaining the covariance relationships. The algorithm would be freely available with a user interface, for evaluation and as a software module that could be used directly in industry.

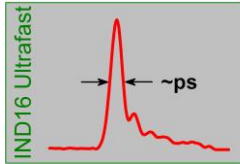
The work was planned as four parts: Investigate the covariance relationships present in the target instrumentation; Design the compression algorithm; Validate the algorithm and write a fast compiled version.

3.2.1: Development of the time-domain/frequency-domain uncertainty propagation algorithm

The aim was to characterise the uncertainty relationships in the time or frequency domain for digital oscilloscope and vector signal analyser instruments and to develop an algorithm to store the covariance results in a compact format. The algorithm had to be fast, space-efficient and capable of handling large data records with $n > 100,000$ points. A key objective was that the algorithm should scale more slowly than n^2 .

The first decision was whether to manipulate and store the results in the time or the frequency domain. The frequency-domain was selected because if the covariance matrix is viewed as a surface then it should be possible to interpolate the data to suit subsequent measurements. Additional benefits were that the result was bounded by the upper frequency limit of the measurement results and convolution is a product in the frequency domain, so measurement contributions could be simply combined.

² D. F. Williams et al., IEEE Trans Microw. Theory Tech. vol. 54, no. 1, pp. 481 – 491, Jan 2006.



The error mechanisms and their effect on the covariance matrix in time and frequency domains using Digital Sampling Oscilloscopes and Digital Real-Time Oscilloscopes (RTDO) were investigated and classified. These results indicated that the dominant correlated contribution from RTDO could be removed by aligning the data in the frequency domain. The algorithm had to be continuous and not limited to the data time-step.

The algorithm planned to compress the results used symmetries within the correlated components to simplify and reduce the storage and processing requirements. This technique was based on the uncertainty analysis of parametric time-correction techniques. The first algorithm developed provided a compression that increased proportional to the number of points and preliminary results. The covariance matrix was designed to maximise visibility of structural relationships by separating the results into their real and imaginary components. The matrix V had the structure:

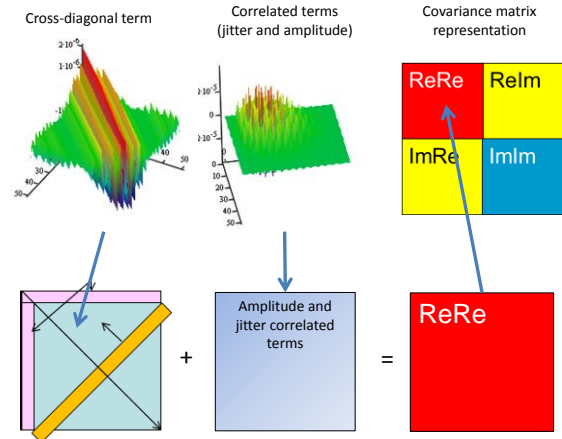


Figure 5: Restructured covariance matrix used for both the symmetry and eigenvalue analysis.

$$V = \begin{pmatrix} V_{RR} & V_{RI} \\ V_{IR} & V_{II} \end{pmatrix}, \tag{2}$$

where $V_{RR}^T = V_{RR}$, $V_{II}^T = V_{II}$, $V_{RI}^T = V_{IR}$, and V_{RR} , V_{II} and V_{RI} are matrices of dimension $n \times n$ containing, respectively, the covariances $\text{cov}(y_i, y_j)$, $\text{cov}(y_{n+i}, y_{n+j})$ and $\text{cov}(y_i, y_{n+j})$ for $i, j = 1, \dots, n$. Each block in the covariance matrix structure showed both correlated and uncorrelated signal components. The uncorrelated terms that appeared as cross-diagonal elements showed some symmetry, allowing the response to be represented by a smaller number of terms, each of length n . The time-error (jitter) and amplitude variation components were highly correlated and could also be represented by single parameters, which could be recovered by a least-squares analysis. The first row and column of each block had to be separately stored as these exhibited different characteristics from the remainder of the matrix.

Data from NPL was encouraging (see Figure 6) with low residual error between the measured and modelled covariance. As part of the internal verification process all the partners were asked to supply data and as a consequence it was found that the algorithm did not work well in all cases and a more robust approach was required.

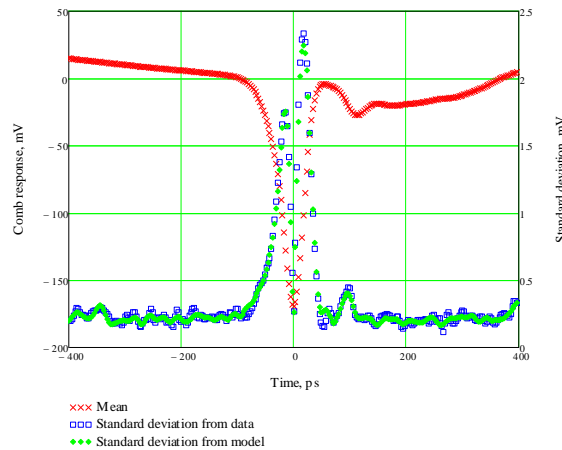
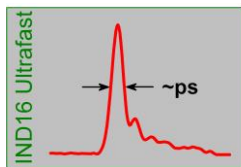


Figure 6: Time-domain response showing mean and standard deviation calculated from the measured and aligned data and from the model using NPL data.

As a consequence of the first algorithm's failure the problem was reassessed and a new algorithm, based on eigenvalue analysis, was developed. It uses the same restructuring of the covariance matrix (Figure 5) that simplifies interpolation. The new algorithm was evaluated using a wider range of datasets with successful results in all cases; and the new algorithm also allows arithmetic manipulation of the results.

As a consequence of the need to extend the algorithm development, work to validate and create a compact compiled version was delayed, but the result was mathematically sound, capable of data manipulation without the need to recreate the full covariance matrix and has the potential for extension to other applications.



3.2.2: Independent validation of algorithm

The objective of this work was to provide an independent verification of the compact covariance algorithm described above. Monte-Carlo Simulation (MCS) was used to provide an independent verification. PTB provided INTA with advice on MCS during the software development.

Supplement 1 of the guide for the expression of uncertainty in measurement (GUM) describes in detail how to use Monte Carlo simulations for uncertainty calculations. The disadvantage of this approach was that the multivariate random number generation as required for MCS is both time and memory intensive. When performing MCS with data records longer than several thousand points, it was necessary to save intermediate results to the hard-disc. These cost penalties meant that MCS was not an easy and quick tool for uncertainty propagation between the time and frequency domains as required by industry and in particular for long record lengths. However, the technique has been used successfully by PTB, where the record lengths are less than 10,000 points.

The key subtasks were:

- Generation of error-simulation model data based on analysis described in Section 3.2.1.
- Algorithm testing and refinement using a Monte Carlo method.

As part of the initial analysis, the impact of different random and correlated processes was modelled to provide a series of known data sets. INTA developed a software tool in Matlab®, `Arbitrary_Pulses_MC.m` that used MCS to generate a series of time domain traces with known impairments. The 'arbitrary' waveforms were defined from the mean traces (in the time domain) obtained from oscilloscope-acquired data files. Subsequently the MC software allowed the user to superimpose three types of contributions (Jitter, Noise and amplitude Noise) so that the set of MC-generated traces could resemble those obtained from real-life oscilloscopes.

The analysis verified the algorithm and investigated the number of simulated measurements, interpolation and undersampling. Subsequently the method of interpolation was changed to provide a realistic result where the uncorrelated uncertainty component is correctly represented. The independent verification demonstrated that algorithm worked satisfactorily.

An unintended consequence of this work was the development of a visualisation tool that showed polar variation of the response. The form of the noise gave some insight into the noise process. This technique may have application for other measurement problems. Figure 7 shows the results using the visualisation tool.

3.2.3: Prototype time-domain/frequency-domain uncertainty software

The aim was to develop an industry optimised, high-speed version of the mathematical software algorithm together with a user interface for evaluation. During this task there was considerable collaboration between VSL and NPL to ensure that the two implementations gave the same result.

The prototype algorithm was translated into Python an object-oriented high-level language so that the algorithm could be evaluated in a licence-free environment by NMIs and industry. This task involved collaboration between NPL and VSL. The Python version of the algorithm was faster, but contained a limited set of features compared with the Matlab® implementation (see Table 1). It subdivided the task into three stages: (a) conversion of the data from time to frequency domain; (b) calculation of the compact covariance; and (c)

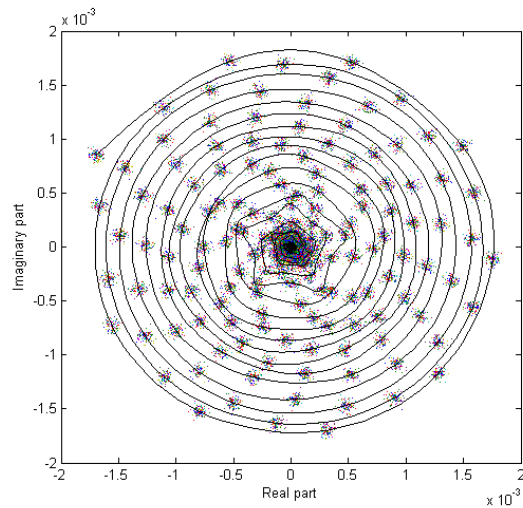
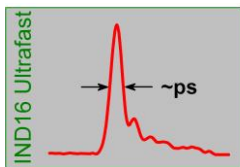


Figure 7: Polar representation tool (100 individual harmonics, mean value in black).



representation of the uncertainty results in the time or frequency domain. The tabulated results are available for further analysis. A screenshot of the dashboard and output plots is shown in Figure 8.

Table 1: Comparison of the features of the Matlab® and Python compact covariance implementations

Function	Matlab®	Python
Fourier transform time-domain results	No	Yes
Calculate compact Covariance	Yes	Yes
Calculate compact covariance for very large files	Yes	No
Addition/Subtraction	Yes	Yes
Multiplication (convolution)	Yes	Yes
Division (deconvolution)	Yes	Yes
Constant	Yes	No
Time-domain response and uncertainties	Yes	Yes
Frequency domain response and uncertainties	Yes	Yes
Frequency interpolation	Yes	No
Run time: 1999 harmonics 41 waveforms	29 sec.	2 sec.

The Matlab® software has been tested using a data set containing 8192 frequency components and the result represented by 7 eigenvalues, giving a compression ratio of over 1000:1.

3.2.4: Release software version

The aim of this task was to extensively test the two software implementations so that a stable release version of the software could be provided free to industry, universities, calibration laboratories and other NMIs.

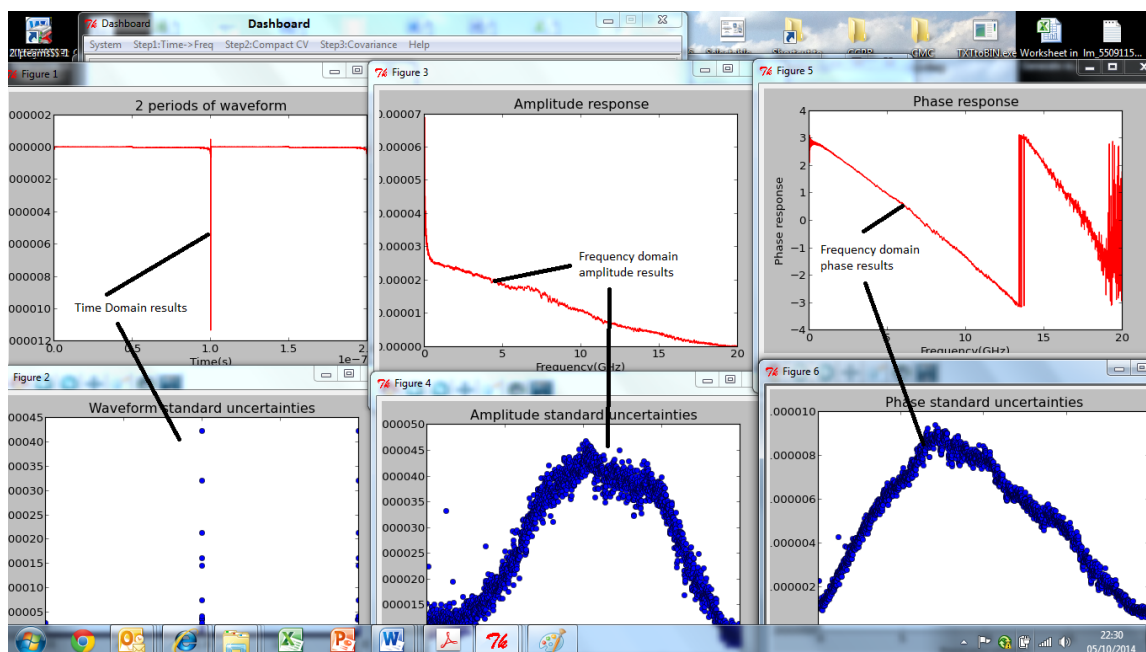
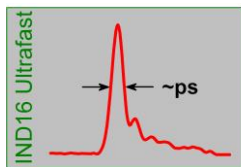


Figure 8: Python desktop showing time and frequency domain results.

All the partners collaborated on this phase of the project. The software and user guide was distributed to the consortium members and a multilingual user interface was implemented to allow for localised language

IND16 Ultrafast



versions. The public release versions of the software and the user guide are available for download through the project website and are hosted at the NPL and VSL websites to simplify maintenance.

To summarise, the compact covariance algorithm was validated by MCS and met the key technical objective of data compression, growing proportional to the number of frequency components. The impact objective of propagating uncertainty results in a resource-efficient way from the primary standard to the factory or lab bench is now possible. An additional benefit is that it is not necessary to create a full-rank covariance matrix, so a smaller number of measured waveforms are required. The algorithm has been realised in both Matlab® and Python (see Figure 8). These are available to the public for free download from the NPL website and through a link from the project website. Details of the algorithm have been published at conferences [8] and a journal publication [18].

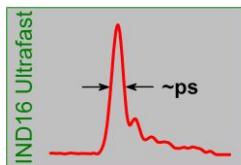
3.3 Investigation of antenna and channel properties in the mm- and sub-mm wave range

The work in this section focused on traceable characterisation of antenna and channel properties in the mm- and sub-mm wave range. It improved the accuracy and the available frequency range of measurements that were needed to characterise the transmission channel and performance of state-of-the-art and future communication and remote sensing systems, including the parameters of antennas which are most important for wave propagation [12]. The work addressed immediate industry needs, as the corresponding measurement capabilities are crucial for the development of new innovative systems. Existing measurement capabilities were limited in frequency and accuracy and were often not available to industry. The few existing measurement capabilities were lacking reliability since they were not traceable to the SI units.

3.3.1: Measurement of gain and directivity diagrams of antennas used in future communication and ranging systems

The aim of this task was the traceable measurement of the gain and directivity diagrams of open-ended waveguides, horn antennas and planar antennas between 40 GHz and 325 GHz and of phased arrays at 60 GHz, 77 GHz, and 94 GHz. The performance of the antennas was evaluated with regard to their suitability for communications and remote sensing applications but also for metrology in channel sounding. Future communication systems that operate at frequencies of 60 GHz and above, as well as remote sensing systems, rely on appropriate antennas. Depending on the scenario, high gain antennas (e.g. paraboloids) that need exact alignment or lower gain antennas that require less steering accuracy are needed. Differentially fed planar antenna structures are gaining more interest in the scientific community since their employment avoids the need of large and lossy balanced-unbalanced (bal-un) structures. For innovative systems (e.g. in an indoor-scenario where a direct line-of-sight path is blocked and a directed non-line-of-sight transmission has to be established or during a radar scan) electronic steerability, as provided by phased-array antennas, is mandatory. While phased arrays are already available at 60 GHz and 77 GHz, only few usable realisations have been presented, mainly due to the difficulties caused by high attenuation and the lack of appropriate phase-shifters. Horn antennas and open-ended waveguides are available for all waveguide bands, as they are used in many scientific applications, but are demanding to fabricate with the required accuracy and hence are expensive in the sub-mm wave bands. Moreover, the metrological characterisation of antennas at frequencies above 40 GHz is inherently difficult due to the physically small but electrically large antenna sizes involved and the non-negligible influence of the measurement equipment and the surrounding setup. Existing setups are often lacking traceability due to non-traceable measurement of the required scattering parameters and insufficient modelling of the external error sources. In the mm-wave range up to 100 GHz, antennas are often characterised in the near-field (spherical or planar scanning) and directivity diagrams are obtained from near-far field transformations whereas at frequencies above that, measurements are quasi automatically in the far-field due to the practical measurement distances. The application of near-far field transformations requires accurate knowledge of amplitude and phase which are often only known with an accuracy of several percent. New more efficient correction techniques to cope with multiple reflections between probe and antenna under test had to be developed in order to improve the accuracy of near-field scanning probe techniques. At high frequencies, existing scanners often measure amplitude only. Here the accurate knowledge of the phase is of benefit e.g. for advanced channel models or for accurate RF localisation techniques.

IND16 Ultrafast



In this task, the capabilities for antenna measurements at very high frequencies were improved. Measurement setups were optimised for gain and directivity diagram measurements between 40 GHz and 325 GHz and uncertainty budgets for the calibration traceable to the SI were set up including the influence from the setup geometry [13,15,28]. These measurements were performed for a variety of antennas that could be used in existing and future communication and remote sensing systems. The choice of approximately 10 to 20 antennas, included horn antennas, open-ended waveguides, planar antennas and phased array antennas at 60 GHz, 77 GHz, and 94 GHz (Figure 9). Especially for the phased array antennas, feeding and beam-forming networks were designed using available simulation software. The measurement results were used to evaluate the performance in future communication systems, as input to channel models applied in Section 3.3.2 and as feedback for optimised antenna design for industrial collaborators. Antenna calibration was also performed for the horn antennas and open-ended waveguides used in the channel measurements of Section 3.3.2.

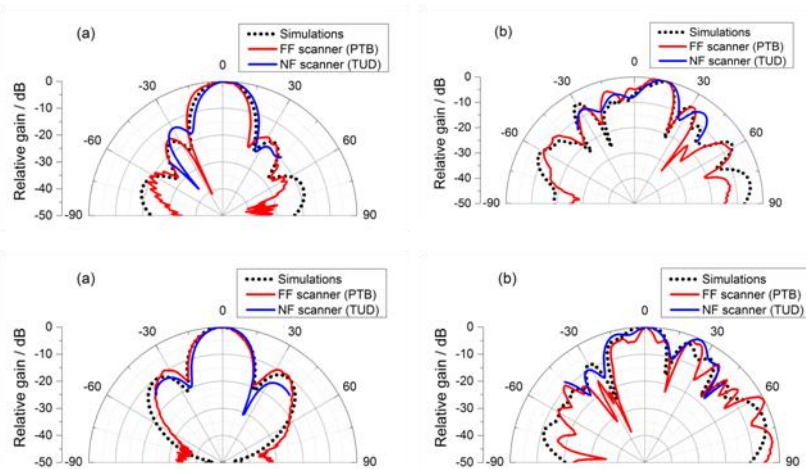
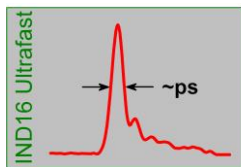


Figure 9: Upper row: Radiation pattern of the 77 GHz antenna array shown in (a) H-plane and (b) E-plane. Lower row: Radiation pattern of the 94 GHz antenna array shown in (a) H-plane and (b) E-plane.

As a major improvement of the measurement capabilities for planar millimetre wave antennas, 4x4 patch antenna arrays for 77 GHz and 94 GHz frequency, including a rectangular waveguide to planar probe transition as test objects, were designed. The arrays were fabricated and then measured using two different measurement systems, a spherical far-field at PTB and a planar near-field scanner at TU Delft. The antennas were designed and optimised using the software CST Microwave Studio, based on the Finite Integration Technique. For frequency matching, a two-stage Wilkinson divider/combiner was included to match the patch impedances to the junction lines. The output radiation of the excitation source was out coupled from the flange to ground layer at the backside of the antenna. There, a rectangle of 2.54 x 1.27 mm² was etched at the WR-10 contact to allow wave propagation from the flange through the substrate and then to the feeding line tip. On top of the antenna front side, a back-short consisting of a quarter-wavelength waveguide and a termination short was placed. A slit was milled from the waveguide along the feeding line to avoid contact between the feeding line and the shim and hence to allow undistorted propagation to the antenna patches. The shim plate thickness and the feeding line cavity width parameter were optimised by including it in the antenna simulation. The shim combined with the short leads to minimisation of the back-reflected radiation into the rectangular waveguide. In the substrate, the shim, and the short precision placement holes were drilled to allow accurate positioning of the antenna on the flange of the frequency converter through the precision pins. In addition to the four precision holes, another three holes were drilled for the screws to tighten the substrate to the flange. The shims and the cover were fabricated with a high-precision computer CNC machine to reduce the mechanical displacement.

An antenna scanner was built at PTB for measuring the antenna radiation pattern in the far-field region within distances up to three meters [30]. It represented a versatile measurement tool required for antenna metrology that was not available at any other European NMI. The scanning system was able to record measurements with high mechanical accuracy where an angular resolution as small as 0.1° was possible. The far-field antenna scanner has two antenna mounts on a rotor arm and on a rail. The antenna under test (AUT) is placed on the rotor arm TX, and the known measuring antenna is placed on the rail RX. The measuring probe is fixed on a track movable up to three meters distance from the rotor arm. The rotor arm is rotatable within an angle from -120° to +120° around the vertical axis. Moreover, both arms are rotatable with an angle from 0° to 360° around the main axis. This allowed measuring the antenna with any possible polarisation. The scanner was installed in a shielded semi-anechoic chamber equipped with absorbers to minimise unwanted reflections and to block external signals. Since the frequency converter modules were

IND16 Ultrafast



placed in metallic boxes, additional absorbers behind the antennas and also surrounding frequency extensions and rotation stages were required. In addition to the antenna arrays at 77 GHz and 94 GHz, a multitude of measurements were performed at an array at 60 GHz (LNE) and at various open-ended waveguides and horn antennas (LNE and PTB). A measurement uncertainty analysis, which was not available before, revealed that VNA measurement errors, cable instability, positioning errors and errors due to standing waves are the main contributors to the overall measurement uncertainty.

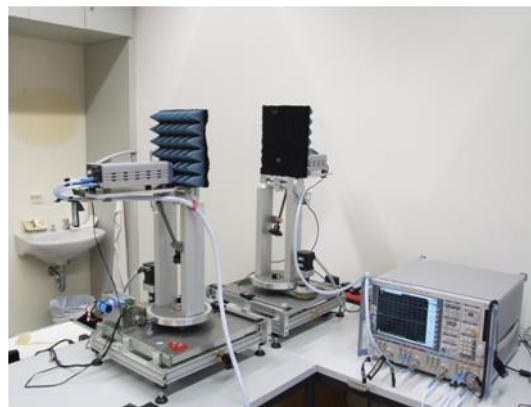


Figure 10: Photograph of the measurement setup.

3.3.2: Channel measurements in typical indoor environments

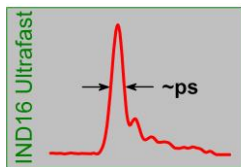
The aim of this task was to perform channel measurements as required for realistic modelling and design of existing state-of-the-art and future communication systems. Impulse responses were determined from frequency resolved transmission measurements in different scenarios where extremely high carrier frequencies between 60 GHz and 300 GHz could be used. As the first communication systems using the 60 GHz band are beginning to emerge, channel measurements for proper system design and performance modelling are needed. However, only preliminary work was performed in this frequency band so far. The existing work did not provide traceability to the SI units. Hence, the reliability of properties obtained within these measurements remained vague. For frequencies beyond 60 GHz, no channel measurements had been performed so far, although many scenarios were conceivable where communication systems could make use of free and unregulated bandwidth available at very high frequencies. In this task, channel measurements with specified uncertainty were performed in a number of representative constellations including kiosk download, office, living room and industrial production environment scenarios for the first time. Angular resolved measurements were performed in the frequency domain using vector network analysers in combination with horn antennas and open-ended waveguides which were calibrated in the work described in Section 3.3.1 [14,16,34]. The channel transfer functions were converted into the time domain yielding the channel impulse response needed for channel modelling. Since the measurements were broadband, the time resolution exceeded that of standard channel sounders working in the time domain. In order to specify possible error sources within the measurements, the measurement equipment, especially the frequency converters used for the upper frequency bands, were characterised comprehensively with regard to unwanted reflections. A unique measurement setup was built according to the requirements of the arranged related scenarios. The frequency converters were placed on mounts rotatable by stepper motors (Figure 10). Standard gain horn antennas, with 20 dB gain each, were attached to the flanges of the rectangular waveguides of the frequency converters. A computer program was written in LabVIEW™ for controlling the stepper motors and for recording the measurements [30]. For the first time, a comprehensive selection of distinct communication scenarios was analysed with large bandwidth.

Communication Scenarios

In a typical desktop download scenario, both Tx and Rx are usually placed on a common table and have a short line-of-sight (LOS) propagation path to each other. Operation on top of a reflecting plane will lead to a remarkable influence according to interference. To investigate this effect a 50 cm long and 60 cm wide metallic plane was placed 5 cm horizontally below the antenna centres. A metallic plane is an almost perfect reflector in the THz frequency range and represents the worst-case assumption for the reflectivity of a table. The channel transmission ($|S_{21}|$) was measured over short distance (~50 cm) with limited scanning angles (from -20° to 20°) of antenna Tx and 1° angular resolution. The measurements were done at positions 15 cm away from each other. The two outer positions, 1 and 3, corresponded to positioning with angular misalignment of communication devices on a table. The measurements covered all the frequencies from 50 GHz up to 325 GHz and there was more broadband than any channel characterisation done before.

One of the most relevant scenarios for future sub-millimetre wave indoor communications is a transmission link within an office room. This implies that both transmitter and receiver establish a directed path for

IND16 Ultrafast



transmission with high data rates over a short propagation distance. The investigated office room contained wooden tables, chairs, wooden cupboards, a metallic door, a glass window and a laptop. Both transmitter and receiver were placed on separate office tables. The mounts were 60 cm high measured from the table surface. The transmission unit was rotated with the aperture of the horn antenna forming a circle with a diameter of about 70 cm. The strength of the received signal may vary depending on composition and position of the objects available in the room. Signals from direct LOS and non-LOS paths are contributing to the measured overall signal. Only the transmitter Tx was scanned rotationally while the reception antenna was kept at a fixed steering. The signal was measured at three different positions of the transmitter.

The next measurement campaign was done in a double-floor room and simulated an industrial environment where bulky metallic and non-metallic objects exist. The area was about 2.5 x 8.5 m² and the height about 5 m. The room included objects such as a metallic switch cabinet, two metallic doors in the ground floor, a wooden cupboard, tables, chairs and metallic stairs that led to a door in the second floor. The Tx and Rx antennas were placed at a side of the room at a distance of about 6.5 m away from each other. The Rx antenna was oriented at three different angles (45°, 0°, -45°) with respect to the plane parallel to the long side of the room. The Tx antenna was scanned angularly by 360°. The network analyser was placed almost at the middle of the room and was connected to the frequency converters via 5 meter cables on each side. This led to a high attenuation of the RF and LO signals, which was critical for the upper frequencies especially the WR-3 band. Therefore, the measurements were restricted to the range from 50 GHz to 220 GHz.

To imitate a living-room download scenario, a room equipped with appropriate furniture was prepared. The room contained tables, chairs, cupboards for books and dinnerware and a flat screen TV. The Tx and Rx were both mounted on rotational units at a distance of 3.1 m from each other. The height of the Tx and Rx was 1.9 m and 0.72 m respectively. The Rx was scanned in 360° and the Tx was placed at some specific angles from 0° - 360° with an increment of 45°. From the magnitude and phase measurements LOS and non-LOS paths were identified successfully as a prerequisite for channel modelling in such an important environment.

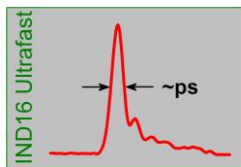
3.3.3: Analysis of diffraction and scattering effects

The aim of this task were measurements on diffraction (edges, objects and humans blocking the beam) and scattering (rough surfaces, hydrometeors) as needed for improved channel models. Realistic channel models have to include diffraction and scattering effects in order to effectively model the wave propagation within a scenario. Many theoretical approaches exist to describe these effects (e.g. the knife edge model to describe diffraction losses or Mie scattering to describe the effect of hydrometeors). However, the applicability of these theoretical approaches is often limited due to the basic assumptions that might not be met (e.g. locally smooth surfaces in the case of Rayleigh scattering from rough surfaces). For the frequency range of interest, theoretical models have often not been verified. In the case of scattering from surfaces, the quality of the theoretical predictions often depends on the accuracy of the material parameters used for the calculations. In the case of free-space propagation which might be disturbed by fumes indoor or by hydrometeors outdoor, propagation characteristics of electromagnetic waves in millimetre wave and in near infrared wave bands were investigated on a long-term experimental basis. Received power level fluctuations are usually monitored on several fixed terrestrial radio frequency (RF) and optical links. Related meteorological parameters that have an influence on the EM wave propagation in the atmosphere are observed simultaneously. Empirical probability distribution functions of EM wave attenuation are obtained as well as the statistics of related meteorological quantities. Based on the measured data and on the EM wave propagation theory, the relationship was modelled between the physical parameters of the atmosphere and EM wave propagation characteristics. Measurements were performed traceable to the SI and the conditions for the applications of the knife-edge method in diffraction, the Rayleigh approach to rough surface scattering and the Mie scattering for hydrometeors were determined with a high accuracy.

Diffraction and Scattering Measurements at LNE

At LNE, diffraction and scattering were analysed in the frequency range from 40 GHz to 67 GHz. The system developed allowed measurements between 33 GHz and 67 GHz using horn antennas in the IEC frequency bands R400 (33 GHz – 50 GHz) and R620 (50 GHz – 75 GHz) with antenna rotating and translating possibility. The propagation was measured on the basis of S₂₁ measurement with a VNA model Agilent Technologies PNA N5227A. This system had been used for the measurement in Sections 3.3.1, 3.3.2, and 3.3.3. Several configurations have been studied either for diffraction or scattering experiments. Different measurements were

IND16 Ultrafast



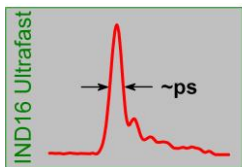
carried out on scattering on rough surfaces with the same system as the one used for diffraction measurements, where one antenna is rotated in order to vary the angle of the reflected beam on the scattering surface. Both vertical and horizontal polarisations were evaluated. The angle of the Rx varied from -10° to 10° around the angular position of the Tx antenna and the magnitude of S_{21} was shown vs. frequency. The highest transmission level was obtained when the antenna angles were the same.

Diffraction and Scattering Measurements at PTB

Measurements were performed using five pairs of frequency extension modules operated with a four-port vector network analyser (R&S ZVA-50) as a source for local oscillator and RF stimulus signal. The frequency converters (R&S ZVA-Z75...325) with output couplers based on rectangular waveguides (WR-15, -10, -6, -5, and -3) were generating and detecting signals in their designated frequency range. The output power of the converters was decreasing with frequency from 4 dBm in the WR-15 band to -20 dBm in the WR-3 band. However, a dynamic range larger than 80 dB was available in all five frequency bands. To imitate diffraction on a person, a living room equipped with appropriate furniture was prepared at PTB. The used room contained tables, chairs, cupboards for books and dinnerware and a flat screen TV. The Tx and Rx were both mounted on rotational units at a distance of 3.1 m from each other at a height of 1.9 m and 0.72 m, respectively. The Rx was scanned in 360° and the Tx was placed at certain angles. From the magnitude and phase measurements LOS and NLOS paths were identified. Additionally, the measurement was repeated under the same conditions while a person blocked part of the beam by standing in the LOS path at a distance of 2m from the Tx and 1.1 m from the Rx. From the magnitude results, it followed that depending on the Tx orientation, signals from indirect paths were observed. It was also noticed that the diffraction decreased while the frequency increased. The reason for this may be that by increasing the frequency, the beamwidth decreased and most of the radiation was passing above the blocking person, hence less diffraction was occurring. These findings have direct impact on a possible system design for indoor communications.

The average scattered power on a certain surface could be calculated according to the so called Kirchhoff approach. To avoid any variation in the electrical properties on the investigated medium surface, homogeneous dielectric materials were produced as a replica from the tested sample surfaces. Nevertheless, in this report scattering measurements are presented as verification with Kirchhoff's model was beyond the scope of this work; however, they were tackled later on. For scattering measurements, the samples were supposed to have a statistical distribution of the surface roughness. Therefore, sandpapers with different surface roughness were chosen to be replicated. The samples were prepared by taking the prints of sandpaper using dentist gypsum called "Silikon Detax Silaplast Futur". This piece was then used to make an image on standard gypsum. This indirect way of producing gypsum images of the sandpaper was to avoid sticking the sand granules in the gypsum and guaranteed bubble-free and homogeneous samples. To avoid diffraction, samples with sufficient size (150 mm x 140 mm) were fabricated. The samples' roughness was measured at PTB using an Alicona Infinite Focus G4. This device measured the optical variation of the beam reflected from the surface of the measured sample to obtain the height profile. From this measurement, the needed information which described the scattered power with respect to the incident power could be obtained. The measurements were performed in a semi-anechoic chamber based on the VNA ZVA-50 from R&S and the corresponding frequency extension units for the frequency range 220 to 325 GHz. For obtaining a parallel beam, lenses were used in front of the horn antennas. The sample was placed on top of a rotatable mount in between the antennas, whereas an absorber was covering the adjacent area to avoid any excessive reflection. The results involved monostatic measurements where only one antenna was scanned and the other was static; and also bi-static measurements where both arms move simultaneously making equal angles with respect to the normal plane. For controlling the scanner a program based on the language LabView™ was written. In bi-static measurements, both the table and the rotor arm moved in a synchronous way such that the Tx and Rx had a uniform angle with respect to the normal plane. The received power was higher than -35 dB in all measurements, which guaranteed a SNR of better than 15 dB. The measurements were performed with standard gain horn antennas with non-perfect linear gain over the frequency range. Antenna gain correction could be done to improve the measurement precision. In monostatic measurements the incidence angle of the transmitter was fixed at 55° and the angle of the receiver at 55° varying by $\pm 5^\circ$. The maximum signal was expected at 55° , which was at the middle of the angle sweeping range. The measurements supported earlier findings, that the Rayleigh approach to rough surface scattering could be applied.

Diffraction and Scattering Measurements at CMI



Propagation of millimetre waves in atmosphere is strongly influenced by molecular absorption, causing frequency selective attenuation, usually called gas attenuation. Gas attenuation is dependent on frequency and on the parameters of air such as pressure, temperature and humidity (expressing the concentration of water vapour in air).

Propagation of mm waves is affected by occurrence of hydrometeors such as rain, snow or hails. An EM wave propagating through the volume of rain is attenuated by means of scattering/absorption on/in water droplets. If multiple scattering is neglected (some simulations suggest that multiple scattering is not very important for propagation of mm waves in rain) the radiation intensity is decreasing with the distance. The absorption coefficient α is proportional to the number of droplets in a unit volume and depends on the extinction cross section C_{ext} of the droplet, which in turn depends on the refractive index of water at the particular frequency and also on the shape and size of the droplet. Here the cross section of the droplet denotes the effective area such that the power of the incident EM wave removed from the beam due to scattering/absorption on/in the droplet is equal to the product of power density of the incident wave and the extinction cross section of the droplet.

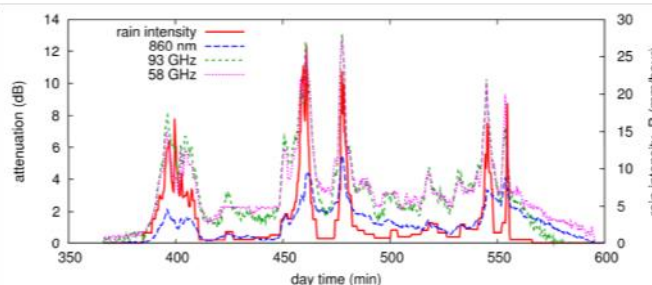


Figure 11: Left: the transmitter site of millimetre wave links, 58 GHz offset parabolic antenna, 93 GHz antenna. Right: example of observed rain attenuation event.

the radiation intensity is decreasing with the distance. The absorption coefficient α is proportional to the number of droplets in a unit volume and depends on the extinction cross section C_{ext} of the droplet, which in turn depends on the refractive index of water at the particular frequency and also on the shape and size of the droplet. Here the cross section of the droplet denotes the effective area such that the power of the incident EM wave removed from the beam due to scattering/absorption on/in the droplet is equal to the product of power density of the incident wave and the extinction cross section of the droplet.

CMI conducted and documented long-term experimental research on the propagation of mm waves in atmosphere. The aim was to obtain reliable statistical data needed for effective design of terrestrial microwave systems operating in mm wave bands. Here, results of experimental research at 58 GHz and 93 GHz on parallel terrestrial paths with the same path length of about 850 m are presented. Two parallel experimental paths between the Institute of Atmospheric Physics of the Academy of Sciences of the Czech Republic (IAP) and the CMI were working at 58 GHz and 93 GHz on a path length of about 850 m. The commercial 58 GHz microwave system operates at 57 650 MHz with V polarisation. The transmitted power was about 5 dBm and the recording fade margin about 24 dB. The commercial 93 GHz microwave system operated at 93 370 MHz with V polarisation. The transmitted power was about 17 dBm and the recording fade margin about 37 dB. An automatic weather observation system was located at CMI near the receiver sites (Figure 11). Rain intensities were measured by the dynamically calibrated heated tipping-bucket rain gauge with collector area of 500 cm². The time of the tips was recorded with an uncertainty of 1 second. Both the records of observed hydrometeor attenuation events on 58 GHz and 93 GHz paths and of rain intensities were statistically processed over a 4-year period. All the recorded individual hydrometeor attenuation events on 58 GHz and 93 GHz paths were compared with the concurrent meteorological conditions and were categorised according to the reasons of their origins as rain, snow, a mixture of rain with snow, a mixture of rain with hail, fog, a mixture of fog with rain a mixture of fog with snow, a mixture of fog with rain and snow.

3.3.4: Analysis of the channel influence on digital signal properties

The aim of this task was a study of digital transmission experiments with different modulation schemes for the scenarios studied in Section 3.3.2. The performance of the transmission had to be evaluated based on traceable digital signal property measurements using the methods developed in Section 3.4. While the operation of communication systems had been successfully demonstrated at 60 GHz, only very preliminary transmission experiments had been performed in the frequency bands above, showing that data transmission in the lower THz frequency range was feasible. In order to further verify the new channel models, digital transmission experiments with high data rates were performed in the scenarios from Section 3.3.2 using a carrier frequency of 300 GHz (Figure 12). Important digital signal properties (e.g. error vector magnitude and carrier-to-noise ratios) were measured for real world communication signals using the methods described in section 3.4. Distance dependent measurements under different propagation conditions (different number of reflections, diffraction, non-specular scattering) were performed to evaluate the channel influence and provided input to Section 3.4 to model the measurement uncertainty [21,35].

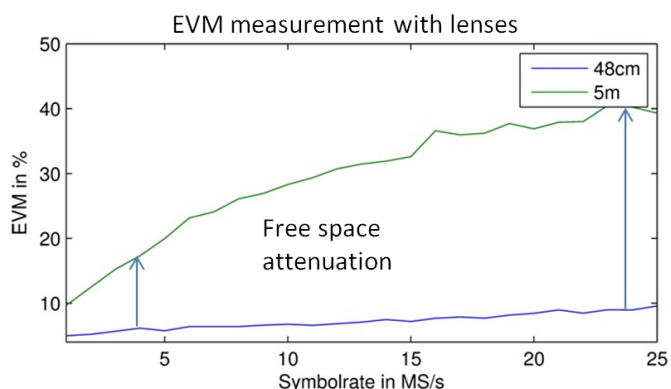
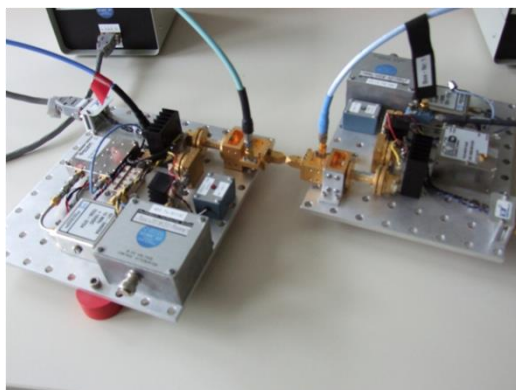
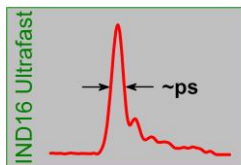


Figure 12: left: 300 GHz measurement system with transmitter and receiver in head-to-head configuration, right: EVM measurement results.

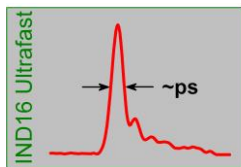
In order to investigate the measurement uncertainty, measurements were also performed based on the determination of the EVM in the time-domain with oscilloscopes. From the experimental results it was obvious that the 300 GHz transmission influenced the quality of the signal. A difference between the EVM measured directly at the output of the generator and at the output of the receiver was observed. The system was able to transmit signals with simple phase modulations (BPSK, QPSK, 8PSK) and more complicated schemes combining amplitude and phase modulation such as 16QAM, 64QAM or 256QAM. The highest distortion was observed for 8PSK and 64QAM modulation schemes. The phase stability of the whole system was only secured when all the generators used a common frequency reference. The system was able to transmit signals with bandwidths up to 10 GHz, yet in this work signals with much lower bandwidths were transmitted. The EVM was measured using a VSA and a method which used a DRTO was shown together with measurement uncertainty. The bandwidth of today's VSAs was not sufficient to analyse signal bandwidths, which could be transmitted using the 300 GHz system. A method using a real-time oscilloscope and consecutive signal processing in a computer was shown, which was not only more open to measurement uncertainty analysis, but also allowed one to measure modulated signals with bandwidths exceeding those of today's VSAs. The phase instability of the received signal due to frequency multiplying and mixing may be significant, which could cause problems especially for modern multicarrier modulation schemes.

3.4 Establish methods for traceable calibration of vector signal generators and analysers and develop tools for a better understanding of the measurement uncertainty of digital signals

The key driver for development of wireless communications is a broadband high-speed data transmission, which demands a "connection always and everywhere". This requires use of new complicated modulation and coding techniques and new hardware solutions with frequencies shifting towards 60-90 GHz. The complexity of measurement instrumentation used for the development and manufacturing of such devices is naturally also increasing. Vector signal analysers (VSA) and vector signal generators (VSG) are the main measurement instrumentation used in the research and development of wireless devices and systems. In order to determine the properties of this instrumentation, a calibration is performed. The term *calibration* in the following text denotes the development of test methods to check the manufacturer's specifications. The measurement traceability is a key requirement of ISO/IEC 17025 for calibration laboratories and instrumentation manufacturers and this was identified as one of the project objectives. In addition to the frequency (amplitude and phase) response of VSAs and VSGs, an unsatisfactory situation existed for the uncertainty propagation of digital signals. Although currently proprietary software is available for use with communications instrumentation to analyse waveforms, this software does not provide any information about the measurement uncertainty. Before the start of the project, EVM could be measured with an approximate error of several percent. In order to design future high speed-communications systems, the EVM needed to be measured traceably with a relative uncertainty in the order of tenths of percent. This would assure a better interoperability of wireless systems and simultaneously reduce development costs.

There has been a clear interest of leading European companies in the research of novel calibration methods and uncertainty of digital signals, which had been expressed by letters of interest (Aeroflex, Agilent

IND16 Ultrafast



Technologies, Anritsu, Catena, Oclaro and others). Based on the needs of the end users, four technical areas were identified which were researched: (a) method for traceable calibration of VSAs; (b) method for traceable calibration of VSGs; (c) uncertainty propagation of digital signals; and (d) traceability for commercial vector signal analysis software.

3.4.1: Traceable calibration of digital-modulation-related functions of VSAs

Today's VSA work with demodulation bandwidths up to 500 MHz (from 2011 to 2014, the state-of-the-art bandwidth increased from approximately 200 MHz to today's 500 MHz). VSAs use various architectures, whereas usually the input signal is sampled in the base band after multiple downconversion using a fast analogue to digital converter with high resolution. The scalar (amplitude) response of the demodulator can be determined with metrological traceability using a calibrated power meter, yet no information about the phase is present due to the principle of VSAs. The strategy for a traceable measurement of amplitude and phase characteristics is using a fast digital sampling oscilloscope (DSO) or digital real-time oscilloscope (DRTO). The DSO is traceable through EOS, which defines the relative timing of the frequency components in the instrument response. Such systems have been developed at several NMIs (NIST (USA), NPL (UK) and PTB (Germany)) (the EOS of PTB was described in Section 3.1).

For characterisation of a VSA, proper broadband signals are needed. Unlike instruments such as a vector network analyser, where the RF source is internal to the instrument and the measurements are of relative phase at different frequencies, a VSA requires a stimulus waveform with multiple frequency components that have known phase relationships to determine the full vector response. The most appropriate option was to use a multisine signal which was easy to generate and had calculable amplitude and phase relations between tones. Multisines consist of several simultaneously generated sinusoids (tones). By changing the relative phase between tones it was able to change the time-domain envelope properties and thus the ratio of the peak and average power (PAPR). The selection of proper multisine signals was done jointly by NPL and CMI using a custom in-house application.

The general principle of the measurement method was to measure the same (multisine) signal from one source by using two different sampling devices. The multisine generator itself was not ideal and thus the signal did not correspond to its mathematical model. The impulse response of the reference device (characterised oscilloscope) was known and the input signal could be removed by deconvolution.

Two different methods of VSA characterisation have been studied in the project. The first one uses a DSO with an auxiliary generator for the oscilloscope's time base correction. Corrected results are unevenly spaced in time so a least-squares approach is necessary to restore an even frequency grid. A negligible inter-sampler jitter is assumed in comparison with the individual channel jitter and one can estimate the relative phase of each measured time point at all three channels. The sampling oscilloscope offers a direct traceability to the EOS, yet it is relatively complicated and not suitable for routine measurements in commercial calibration laboratories. The other method for VSA vector response characterisation uses a DRTO. A time-base correction technique is now needed which utilises the pilot signal with carrier frequency different from the frequency of the multisine signal.

The measurements were performed by NPL, PTB and CMI with set of different measurement instrumentation at different locations. Two measurement examples are given in this report. The first was using a DSO which is directly traceable to the EOS. A multisine signal with low PAPR was used. This signal was captured both by a DSO (20 GHz bandwidth) and VSA (15 MHz bandwidth). The amplitude and phase responses of the VSA after deconvolution of the measured multisine signal are shown in Figure 13.

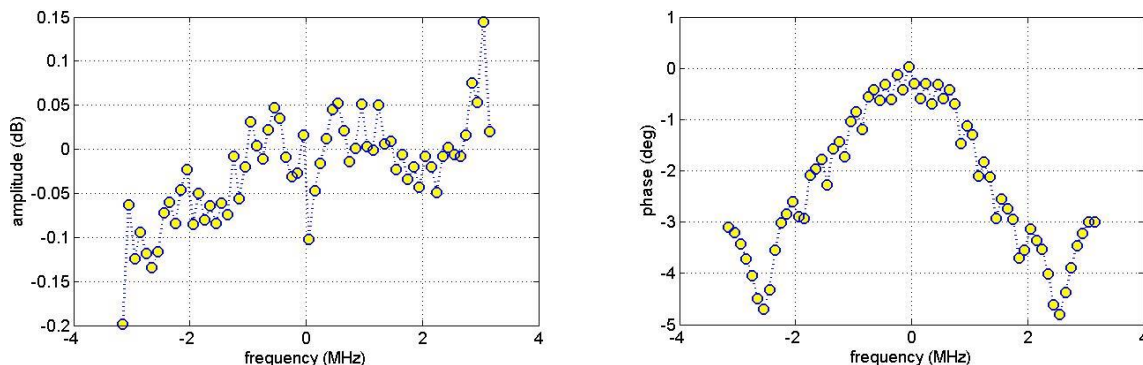
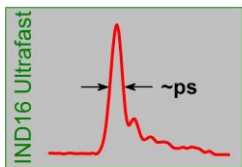


Figure 13: Amplitude (left) and phase (right) response of the VSA after deconvolution of the measured multisine signal.

The second example shows an experiment with a VSA and a DRTO with bandwidth of 2.5 GHz. The multisine carrier frequency, pilot tone frequency and DRTO's sampling rate were chosen properly in order to be able to correct the DRTO's time base. The VSA demodulation bandwidth was 40 MHz. The multisine was generated using an arbitrary waveform generator and upconverted to a carrier frequency. A pilot signal with frequency different from the carrier one was used. The multisine reverse polynomial phase profile and cosine phase profile were artificially created. Figure 14 shows the comparison of VSA and the DRTO amplitude response for the signal with low PAPR (polynomial phase profile).

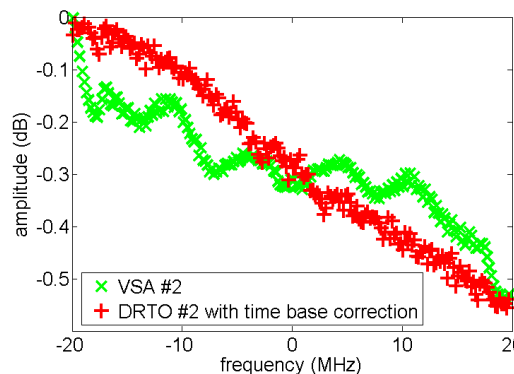


Figure 14: Measurement of a multisine signal with PAPR ~ 2.6 dB.

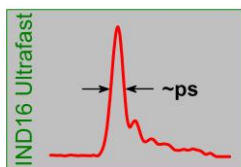
Currently NMIs offer a calibration of DSOs' transfer function, whereas 500 MHz frequency spacing is available traceable to the EOS system. The knowledge base for the uncertainty of the DSO transfer function was provided by PTB and NPL. The type A uncertainty can be calculated from many repeated measurements using the compressed covariance approach introduced in Section 3.2. The main Type B uncertainty contributions are the impedance mismatch, oscilloscope's time base correction and noise contribution of the oscilloscope and also the hardware impairments, which were studied by VSL.

The achieved results can be used by commercial calibration laboratories, provided a DSO or DRTO with full traceability is available (transfer function). The methods developed in this section have not been used in industry so far and represent a progress beyond the state-of-the-art. Currently the frequency step of the DSO transfer function is approximately 500 MHz but it is expected to achieve smaller frequency spacing through use of a modified EOS setup. The method is convenient for future VSAs operating in the frequency band 60-90 GHz. A series of inter-laboratory comparisons is needed to offer this measurement as an accredited service. A calibration guide has been issued jointly by CMI, NPL, VSL and PTB, which gives users practical recommendations on how to calibrate a VSA.

3.4.2: Traceable calibration of digital-modulation-related functions of VSGs

Modern VSGs are able to create modulated signals with bandwidth of about 2 GHz (communication signals, multitone signals, radar signals, etc.) with use of an arbitrary waveform generator. This baseband signal is then upconverted to the carrier frequency. There are many parameters to check during the instrument's calibration –frequency, power, analogue modulations, etc. – and there exist methods traceable to standards of higher precision. For quality of modulated signals, such traceable methods did exist before the start of the project. In the framework of the project, a method which uses waveform metrology for determining properties of modulated signals was developed.

IND16 Ultrafast

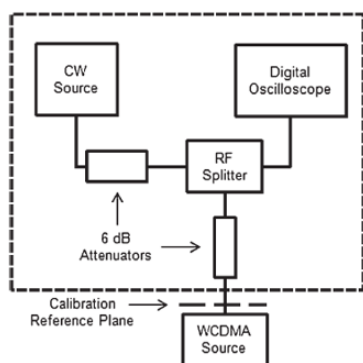


For characterisation of the quality of a modulated signal, each manufacturer uses its own method. Usually a VSA is used, the source is characterised using an analyser and vice versa, which forms a closed calibration loop. The method developed in this project now breaks this loop.

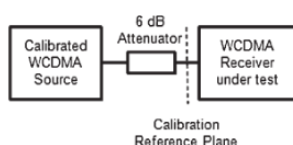
The digitally modulated signal is represented by two low-frequency orthogonal signals, the so-called in-phase (I) and quadrature (Q) component. If we plot them together into one diagram and select only samples at ideal positions, we obtain a constellation diagram. The error vector magnitude (EVM) is defined as a ratio of the sum of magnitudes of error vectors and ideal vectors.

The traceable EVM characterisation consists of using a fully characterised sampling device (which is an oscilloscope or a VSA with full traceable vector response). The second step is signal processing and demodulation using a validated method, which means open access to all calculation steps and evaluation of errors. This can be achieved using waveform metrology, where a measurement uncertainty is attributed to each measured point in the time or frequency domain. For demodulation of the signal, freely available software was developed by CMI and MIKES in the framework of the project (see Section 3.4.3). Different sampling devices were also studied.

The DSO is a well characterised sampler with direct traceability to the EOS, yet it is not convenient for EVM measurements due to very long acquisition times and restrictions on the type of modulated signal to measure, as shown by NPL. On the opposite side, a DRTO is frequently used in commercial calibration laboratories and allows measurement of long signal epochs and non-periodic signals. However, there are several drawbacks, such as the low vertical resolution (typically <8 bits) and complicated internal structure of the analogue to digital converters.



source calibration



analyzer calibration

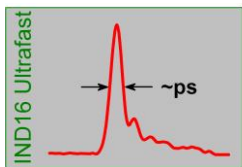
A DRTO transfer function (traceable to EOS and DSO) was needed for the correction of the measured signal (application of an inverse filter to equalise the frequency characteristics of the measured waveform); and an example of the determination of the EVM of the source and receiver separately was demonstrated by NPL. First, the WCDMA source was characterised using a DRTO (see Figure 15). The auxiliary CW generator was for the oscilloscope's time base correction. The EVM of four different receivers was then compared.

Figure 15: Source and receiver calibration.

Another measurement option was to use a characterised VSA. Measurements are very quick and user-friendly, yet the VSA measurements lacked measurement traceability. However, a method for traceable characterisation of the VSA's transfer function was described in Section 3.4.1 of this report. The modulated signal measured by the VSA was then corrected with the knowledge of the VSA's transfer function. A number of experiments were performed by PTB, CMI and NPL using different sources and sampling devices. Various symbol rates were chosen and the carrier frequencies were chosen so that they did not fall into any mirror or spurious product in the spectrum.

As a demonstration of the EVM change with ambient conditions, a VSA and DRTO were placed in a climatic chamber and the EVM was measured by MIKES. The temperature range was 15 °C to 35 °C. Only very slight influence of the temperature to the resulting EVM was observed (the RMS value of EVM increased by approximately 0.2 % after increasing the temperature from 15 °C to 35 °C). Signals with different modulation schemes and symbol rates signals were studied; and the results were incorporated in the final user guide.

Experiments with the VSA were performed by CMI and PTB with specialised expertise from NPL. Different sets of measurement instrumentation from different vendors were used with the aim to check the generator's digital signal quality. The measured base band waveforms were corrected for the VSA's IQ demodulator frequency response or oscilloscope's transfer function, the EVM was calculated from the IQ baseband signal and then analysed using the software created in this project. Signals with different symbol rates, different



modulation schemes and different result lengths were analysed. The EVM uncertainty evaluation is a complicated process with many unknowns. Basically, there is one input (waveform measured by the oscilloscope with thousands to millions of samples), subsequent signal processing (comprising mainly carrier removal, phase offset correction, frequency offset correction, filtering and amplitude scaling) and one output (the EVM value, one number). The most complicated problem was to propagate the uncertainty from the source (generator) through the measurement device (oscilloscope, VSA) and subsequent signal processing to the uncertainty of the resulting EVM value and to distinguish between the influence of the generator itself and the transmission system and measurement device to the EVM.

The results of this task will be used for a traceable characterisation of VSGs at NMIs and commercial calibration laboratories. The method uses a traceable oscilloscope or a VSA and validated demodulation software. A calibration guide was issued jointly by CMI, NPL, VSL and MIKES, giving users practical recommendations on how to calibrate a VSG.

3.4.3 Uncertainty propagation of digital signals

The EVM calculation in a general signal analyser has several processing steps: 1) down-conversion of the signal to an intermediate frequency; 2) the signal is sampled using a fast A/D converter; 3) systematic errors are eliminated; 4) the signal is demodulated based on the standard used; 5) original bits are restored; 6) ideal signal replica is created; and 7) the EVM is calculated. When using an oscilloscope, the down-conversion is performed in a computer and the signal is sampled directly at the RF carrier frequency. The problem lies in the elimination of systematic errors. In 3GPP standards, no exact method is determined so analysers from different vendors may give slightly different results. A mathematically rigorous method was implemented in the software created by CMI and MIKES within this project. The first Matlab® prototype developed by CMI resulted in the executable version based on C++ environment, which was developed by MIKES. Both applications can be downloaded from the project website and screenshots are given in Figure 16. The application is also able to calculate measurement uncertainty with use of the compressed covariance matrix approach extended to complex numbers. This is a progress beyond the state-of-the-art. The application is free of charge.

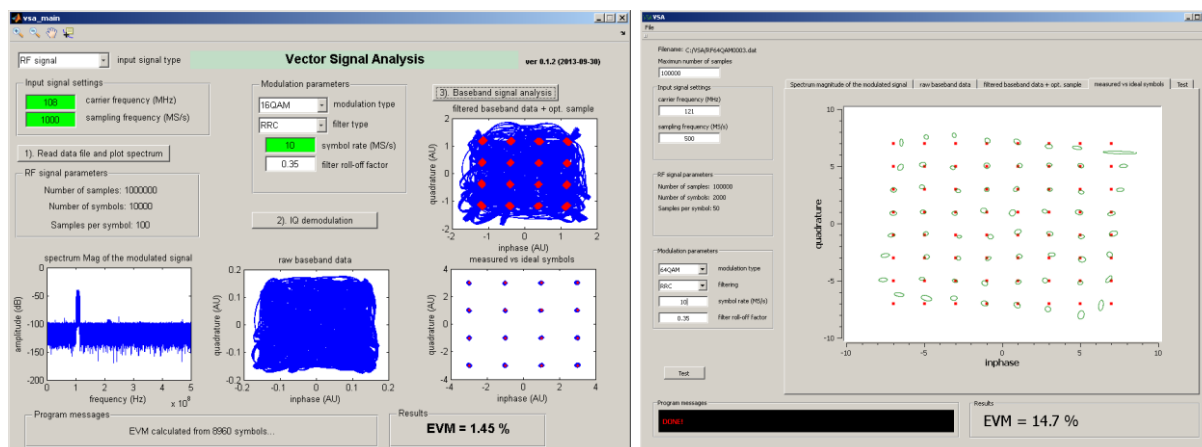
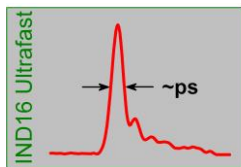


Figure 16: Software applications for EVM uncertainty calculation (MATLAB, left, and C++, right).

3.4.4 Traceability for commercial vector signal analysis software

There exist many applications for EVM calculation from different vendors, either as separate PC software, or as firmware options in measurement instrumentation. The commercial packages, however, do not have direct access to the computational process and the user cannot determine the measurement error. One such software package, loaned by Agilent Technologies, was studied in the project by VSL, with expertise from NPL and Agilent. Digital signals with known properties were generated and stored in data files compatible with the demodulation software and served as reference data. Reference data was generated using Matlab® File Builder (MFB) developed in the project by VSL. To investigate the EVM, magnitude error and phase error measurement functions, a set of reference data was analysed by the VSA software, hence allowing precise evaluation of the VSA software under test.

IND16 Ultrafast



Thorough testing of the software was performed using signals with known (calculable) EVM with dependency on the signal level, filter roll-off factor, number of symbols, sample rate, etc. The results were the maximum and minimum measurable EVM (EVM noise floor). Modulation techniques with larger number of symbols in the constellation diagram are more sensitive towards noise and therefore also have much lower maximum measurable EVM threshold.

To ensure thorough testing of other software packages, detailed insight to the software internal functions is needed and this requires close cooperation with the software vendor.

4 Actual and potential impact

4.1 Societal benefit

The societal benefit, identified by the EC is “The steady increase of the bandwidth of new communication systems and remote sensing applications continuously improves the quality of life of many people worldwide.” This is a very high-level objective and the issue is whether presence or absence of this project would make a difference to the quality of life of European citizens. When preparing this project it was identified that there were unsolved waveform metrology challenges where an impact could be made as these deficiencies currently hinder research and development of high-frequency devices in Europe, which in the longer term affects the development and roll-out of new systems within Europe. The telecommunications and electronics sectors are high-value, in terms of employment, and the infrastructure that they underpin has been identified as important for wealth-creation within Europe. This project provided the tools to extend dynamic waveform traceability and uncertainty analysis to industry in a useable form.

4.2 Strategic approach to impact within this project

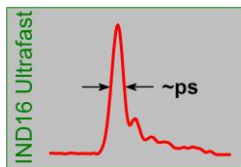
The strategy identified to maximise the impact of this project was a combination of top-down and bottom-up approaches. The electrical waveform primary standard, based on electro-optic sampling (EOS), is the focal point of the metrology chain. The top-down aspect of this project was to reduce the uncertainties of the EOS system (see Section 3.1) and to improve the dissemination of the results and their uncertainties (see Section 3.2) so that commercial calibration laboratories have the ability and algorithms to apply the uncertainty results to their own measurement. This will greatly increase the fan-out of the uncertainty data to industry. The impact should cover the whole electronics sector as the traceably calibrated equipment can be used in many technology areas.

The bottom-up approach comprised of three strands: mm-wave Over-the-air (OTA) measurement of room environments (see Section 3.3); support and analysis tools for communications waveforms (see Section 3.4) and a dissemination strategy (Section 4) that covered industry, academia and practicing engineers. To achieve breadth of dissemination “local language” presentations were introduced, many of which included a training element, so that the research findings were disseminated to engineers and scientists less likely to have the opportunity to attend major conferences. Similarly, research findings were published in trade journals, which have a wide distribution (typically >5000 physical copies + online).

Additional opportunities to stimulate impact were also identified during the project. There is considerable interest in OTA measurements and the measurement of different environments within research communities such as COST 2100 and IC1004 and through standards bodies such as ETSI and CTIA. Much of the measurement work in these communities is carried out by students with excellent technical skills, but no grounding in metrology. Interaction with them has enabled the NMI community to understand the issues (e.g. training needs) so that greater leverage for good practice can be provided.

The compact covariance software (see Section 3.2), that will traceably disseminate waveform results from the primary standard, may also benefit a number of other science areas, such as spectroscopy, that capture waveform data.

IND16 Ultrafast



4.3 Dissemination activities

Knowledge transfer is the main method to help industry develop a greater understanding of metrology issues. The scientific results have been mainly disseminated through scientific publications in peer reviewed journals and through presentations at conferences and workshops. In addition, conformity standards provide a stimulus for the use of better measurement capabilities. The key dissemination methods used in this project were:

1. Standards committees: These have an immediate impact on industry. The project participated in five separate standards committees comprising two international (IEC TC 85, IEEE 802.15) and three national (DKE/UK 767.4, DKE/K964, VDI/VDE-GMA FA 8.17) standards committees.
2. Scientific publications in peer-reviewed journals: nine peers-reviewed journal papers were submitted and in the 6-months following the end of this project, an additional five peer-reviewed publications will be submitted.
3. Scientific publications in (preferably) peer-reviewed conferences: excluding workshop presentations, a total of thirty-four oral or poster presentations were made at international conferences.
4. National (local language) meetings: Local-language meetings or training activities were organised by each participating national measurement institute (one per NMI, per year) and these included a higher training element than can be achieved through traditional presentations. The local meeting impact on scientists and engineers who are less likely to attend the international meetings. The events run by CMI typically attracted 80 participants
5. Workshops: Overall seventeen presentations were made at four workshops. The attendance ranged from 20-60.
6. Trade journals: three papers have been submitted to trade journals and a further paper is in preparation.
7. Training: The workshops contained a training element and overall sixteen training activities, including three for project members, were undertaken and an additional training event is planned.
8. User guides: Seven user guides, covering all technical areas of this research project have been written, which will be disseminated to users at industry, calibration laboratories and National Metrology Institutes. More detailed information is given in User Guides when compared with technical papers so we expect that impact from the user guides will be significant. Also, the IP is owned by the NMIs so the user guides will be available for free download from the website.
9. Newsletters: Two newsletters were released during the lifetime of the project and a final newsletter will be released shortly.
10. Downloadable software: the key software products developed in sections 3.2 and 3.4 can be freely downloaded from the project and NMI websites.

Overall, the project members gave 53 presentations at national and international conferences, submitted 3 trade journal papers and undertook 16 training activities. In the 6-months following the end of this project, 5 additional peer-reviewed publications will be submitted.

4.4 High-profile events and awards

Project members gave plenary talks at the International Conference on Infrared, Millimeter and Terahertz Waves 2013 (Thomas Kleine-Ostmann, "THz metrology") and Conference on Precision Electromagnetic Measurements 2014 (Mark Bieler, "The femtosecond laser as a microwave instrument"). With audiences of more than 300 people both of these talks reached a wide community.

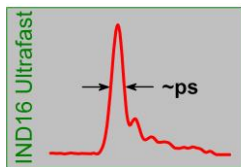
Project members received the CPEM 2012 Early Career Programme Award (Martin Hudlicka, CMI, for work described in section 3.4) and the 3rd place of the Student award at the IRMMW-THz Conference 2012 (Heiko Füsler, PTB, for work described in Section 3.1).

4.5 Workshops

The two key workshops took place at the European Microwave week conferences (2012 and 2013) and a third was organised at VSL.

The first workshop W09 at European Microwave Conference 2012, "Why professional LSNA, NVNA, scope and VSA users care about accurate phase information" was organised by Frans Verbeyst (REG1 home

IND16 Ultrafast



organisation) through the IEEE MTT-11 (TC33) group. The meeting room accommodated the 20 participants. The standard of questions was high.

The second workshop W31 was held at European Microwave Conference 2013 “Do You Have Confidence in Your RF Waveforms? Developments in Waveform Metrology and Uncertainty Propagation for RF and Digital Signals” was organised by the project coordinator. The workshop covered all objectives of this research project and showed the main project highlights at that time. It was an opportunity to discuss the results dissemination for future applications. The PDF presentations have not only been available to the workshop participants, but also to a wide range of other experts who attended other conference workshops (all the presentations have been available on one common USB stick).

A workshop on Digital Signals has been organised by VSL in Delft, The Netherlands, in June 2014. One talk summarizing this research project and seven technical talks have been given.

4.6 Exploitation and uptake

The project had 8 collaborators and 20 stakeholders from outside the NMI community. Collaborators mainly provided advice to the consortium to focus the activities and maximise the industrial impact.

The outputs of the project will improve calibration and measurement services at the NMI level. This includes ultrafast waveform measurements, but also measurements of digital signals. For example the calibration services at PTB and NPL for the time response of ultrafast sampling oscilloscopes will be enhanced using results from the project. Additional possible calibration services may range from improved antenna characterisation for future communications systems to the characterisation of vector signal analysers and vector signal generators. In time, commercial calibration laboratories may uptake some of the results and offer new services such as traceable calibration of vector signal generators and analysers for wireless communications. Project results have been shared with two stakeholders. A clear answer on uptake of the results has not been obtained from these companies, as certain internal processes and procedures are confidential. However, project partner Agilent UK (now Keysight Technologies, with headquarters located in Santa Clara, USA) are one of the leading-edge manufacturers of Signal Analysers, Signal Generators and Conformance Test Solutions for the wireless communication industry. Both the commercial calibration laboratories and Keysight Technologies have already expressed the project results as very helpful for their future work.

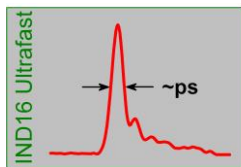
There has also been interest in evaluating the covariance software from two NMIs outside the project, including INTI (Argentina). It can be expected that this number will significantly increase once all submitted journal papers have been published. In the longer term NPL plan to disseminate waveform calibration results using this software and provide a copy of the software to users of the calibration service. The users of the current calibration service mainly comprise calibration laboratories and NMIs, although there are also manufacturers selling the equipment with a calibration report. Thus, potential certainly exists in making some of the state-of-the-art instrumentation and algorithms developed within the project commercially available.

An important exploitation area is expected to be consultancy and advice on calibration of high-frequency instrumentation to industrial partners and other national metrology institutes and laboratories.

The uncertainty propagation software has already been used in further research projects, such as the EMRP project IND51 “Metrology for optical and RF communication systems”, suggesting that impact can also be achieved in other fields. An unexpected consequence of the work on the uncertainty algorithms is that they provide significant benefits in other technical areas, such as THz spectroscopy. Applying the analysis technique to the data from these instruments has provided an improvement of $\times 79$ to the uncertainties [24]. These measurement systems are used to characterise material properties and have been used to identify material content and structural properties, which has the potential for applications such as fraud detection. Good performance and uncertainties are important for such an application to increase confidence in the result. We anticipate that there will be future impact generation through other applications.

Members of the project directly contributed to a new standard on the calculation of waveform parameter uncertainties (IEC TC 85, WG22). This standard is expected to be completed in 2015 and is applicable to all industries that generate, transmit, detect, receive, measure, and/or analyse step- and impulse-like waveforms.

IND16 Ultrafast



4.7 Contribution to longer-term impacts

The results from this research project are centred on the measurement of waveforms used in ultrafast electronics and increased cooperation between the NMIs involved. The uptake of the new measurement capabilities available at NMIs by the calibration and instrumentation sector will over time lead to longer-term economic, environmental and social impacts likely to be secondary effects.

The economic impact will be created via by technology developments in ultrafast electronics and modern wireless communications. The communications industry represents a multi-billion euro market and errors in testing might cause additional expenses to manufacturers of high-volume electronic devices.

The long-term impact for the environmental and health sector will be through improved design of RF components and systems that will help to decrease transmitted power: In order to reduce energy consumption, microwave and integrated circuits are nowadays driven beyond their linear mode of operation. This requires the exact characterisation of the time or frequency behaviour of these circuits and such measurement techniques have been developed in the project.

Millimetre-wave RF communication links are a possible option for last-mile (few hundred metres) delivery of broadband signals. mm-wave communication will be important for 5G development and outputs from the project have highlighted measurement issues in this area and may underpin future work.

Society may also benefit from the project as it will help to ensure availability of information at any place and at any time. Wireless communication systems use a variety of advanced modulation and coding techniques in order to increase the data rates and to make the links more reliable and robust. The traceable characterisation of corresponding measurement devices has been studied in this project.

We have already found that the mathematical algorithms developed in this work can have benefits in fields outside the current research area. We speculate that the techniques may be applicable in many areas where the results are in the form of a waveform and where correlated errors occur in the data.

4.8 Effective cooperation

The cooperation between the project partners was effective and produced many joint presentations and publications. The different experience and instrumentation available at particular NMIs led to joint research results, which could not be achieved by single NMIs alone. The metrology, and particularly, industrial communities will profit from the joint research as it provides more unbiased results than could be achieved by a single NMI. During all three organised workshops, several technical talks with results originating from this research project have been given; and many video conferences or personal meetings took place to discuss technical issues.

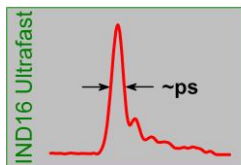
Some examples for effective cooperation activities are listed below:

- PTB and NPL finished a comparison of ultrashort voltage pulse measurements using laser-based electro-optic sampling techniques.
- Joint measurements were performed by CMI and PTB to better characterise a real-time oscilloscope.
- PTB and TU Delft cooperated on the characterisation of planar array antennas at 77 GHz and 94 GHz. PTB designed the antennas and measured the radiation patterns in the far field and TU Delft measured the near field radiation patterns.
- INTA and NPL are collaborating to publish the visualisation techniques developed in this project. Data exchange and analysis is planned between PTB and NPL and possibly also between VSL and NPL.
- PTB gave training to LNE staff on electro-optic sampling.
- The uncertainty propagation software was distributed to all partners and a multilingual user interface was implemented by all partners to allow for localised language versions.

5 Website address and contact details

Project website:

www.ptb.de/emrp/ultrafast.html

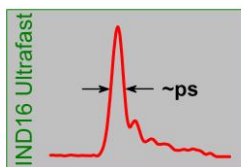


Project coordinator:

Dr. Mark Bieler
Physikalisch-Technische Bundesanstalt
2.54 Femtosecond Measurement Techniques
Bundesallee 100, D-38116 Braunschweig
Germany
phone: +49-531-592-2540
fax: +49-531-592-69-2540
email: mark.bieler@ptb.de

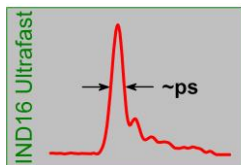
6 List of publications

- [1] Martin Hudlička, “Metrology of digitally modulated signals”, *Metrologie*, Vol.21, 2012, pp. 11-15.
- [2] D. Humphreys, M. Akmal, “Channel timebase errors for Digital Sampling Oscilloscopes”, *Digest on Conference on Precision Electrical Measurements 2012*, DOI: 10.1109/CPEM.2012.6251032 pp. 520 – 521.
- [3] P.D. Hale, D.F. Williams, A. Dienstfrey, J. Wang, J. Jargon, D.A. Humphreys, M. Harper, H. Fuser, M. Bieler, “Traceability of high-speed electrical waveforms at NIST, NPL, and PTB”, *Digest of Conference on Precision Electrical Measurements 2012*, DOI: 10.1109/CPEM.2012.6251033 pp. 522 – 523.
- [4] D. Humphreys, J. Miall, “Traceable measurement of source and receiver EVM using a Real-Time Oscilloscope”, *Digest of Conference on Precision Electrical Measurements 2012* DOI: 10.1109/CPEM.2012.6250685, pp. 110 – 111.
- [5] M. Hudlicka, C. Jastrow, T. Schrader, T. Kleine-Ostmann, “Waveform metrology for error vector magnitude measurements in a 300 GHz transmission system”, *Digest of Conference on Precision Electrical Measurements 2012*, DOI: 10.1109/CPEM.2012.6251035, pp. 526 – 527.
- [6] Wei Tian, D. Allal, G. Boudebs, M. Charles, O. Ndiaye, P. Vincent, “Development of an electro-optic sampling system at LNE”, *Digest of Conference on Precision Electrical Measurements 2012*, DOI: 10.1109/CPEM.2012.6251099, pp. 654 – 655.
- [7] David Humphreys and James Miall, “Traceable Measurement of Source and Receiver EVM using a Real-Time Oscilloscope”, *IEEE Trans Instrumentation and Measurement*, No. 62, Vol. 6, 2013 pp. 1413-1416.
- [8] D.A. Humphreys, P.M. Harris, J.M. Miall, “Instrument related structure in covariance matrices used for uncertainty propagation”, *Proceedings of the 42nd European Microwave Conference*, Nov. 2012, pp. 1304 – 1307.
- [9] Martin Hudlicka, Mohammed Salhi, D.A. Humphreys, “Towards Metrological Characterization of Vector Signal Analyzers”, *Proceedings of the 42nd European Microwave Conference*, Nov. 2012, pp. 558 – 561.
- [10] M. Bieler and H. Fuser, “Realization of an ultra-broadband voltage pulse standard utilizing time-domain optoelectronic techniques,” in *Proc. SPIE 8624, Terahertz, RF, Millimeter, and Submillimeter-Wave Technology and Applications VI*, 2013, pp. 862417.
- [11] H. Fuser and M. Bieler, “Frequency, amplitude, and phase measurements of GHz and THz sources using unstabilized THz frequency combs,” in *Proc. SPIE 8624, Terahertz, RF, Millimeter, and Submillimeter-Wave Technology and Applications VI*, 2013, pp. 86240T.
- [12] Thomas Kleine-Ostmann, “THz metrology”, *Digest of 38th International Conference on Infrared, Millimeter, and Terahertz Waves (IRMMW-THz)*, Sep. 1-6, 2013, DOI 10.1109/IRMMW-THz.2013.6665913.



- [13] M. Salhi, T. Kleine-Ostmann, and T. Schrader, "Design and characterization of 4x4-phased-array patch antennas at 77 GHz and 94 GHz", Digest of 38th International Conference on Infrared, Millimeter, and Terahertz Waves (IRMMW-THz), Sep. 1-6, 2013, DOI 10.1109/IRMMW-THz.2013.6665641.
- [14] T. Kleine-Ostmann, M. Salhi, M. Kannicht, S. Priebe, T. Kürner, and T. Schrader, "Broadband Channel Measurements between 50 GHz and 325 GHz: Comparison of Different Propagation Scenarios", Digest of 38th International Conference on Infrared, Millimeter, and Terahertz Waves (IRMMW-THz), 2013 DOI 10.1109/IRMMW-THz.2013.6665493.
- [15] Mohammed Salhi, Carolin Peiss, Michael Botschka, Thomas Kleine-Ostmann, and Thorsten Schrader, "Characterization of 4x4 Planar Antenna Arrays for the Frequencies 77 GHz and 94 GHz Using an Antenna Scanning System", Asia-Pacific Microwave Conference Proceedings (APMC), 5-8 Nov. 2013, pp.1106 – 1108, DOI 10.1109/APMC.2013.6695036.
- [16] M. Salhi; T. Kleine-Ostmann, M. Kannicht, S. Priebe, T. Kürner; T. Schrader, "Broadband channel propagation measurements on millimeter and sub-millimeter waves in a desktop download scenario", Asia Pacific Microwave Conference Proceedings (APMC), 5-8 Nov. 2013, pp. 1109 – 1111, DOI: 10.1109/APMC.2013.6695037.
- [17] Heiko Füsler and Mark Bieler, "THz frequency combs", Journal of Infrared, Millimeter, and Terahertz Waves, vol. 35, pp. 585–609, 2014, DOI: 10.1007/s10762-013-0038-8.
- [18] David Humphreys, Peter Harris, Faisal Mubarak, Dongsheng Zhao, Manuel Rodríguez-Higuero and Kari Ojasalo, "Principal Component Analysis Compression Method for Covariance Matrices used for Uncertainty Propagation", IEEE Trans Instrumentation and Measurement, submitted Jan 2014, available (early access) at <http://ieeexplore.ieee.org/Xplore/home.jsp>.
- [19] M. Hudlicka, D. A. Humphreys, F. Mubarak, M. Salhi, "How to characterize vector response of future broadband instrumentation, Microwave Engineering Europe, February 2014, online issue, available at http://www.tm-eetimes.com/en/how-to-characterize-vector-response-of-future-broadband-instrumentation.html?cmp_id=71&news_id=222918833.
- [20] Martin Hudlička, David A. Humphreys, Mohammed Salhi and Faisal A. Mubarak, "Characterise vector response of broadband instruments", EE Times-Asia, Download available at http://www.eetasia.com/STATIC/PDF/201403/EEOL_2014MAR18_TEST_NET_TA_01.pdf?SOURCES=DOWNLOAD.
- [21] M. Hudlicka, M. A. Salhi, T. Kleine-Ostmann, T. Schrader, "Characterization of a 300 GHz Transmission System for Digital Communications", IEEE Trans. on Terahertz Science and Technology, submitted in April 2014.
- [22] Kari Ojasalo, Martin Hudlicka and David A. Humphreys, "Uncertainty of communication signals measurement", Digest of Conference on Precision Electrical Measurements 2014, 24th August 2014, pp. 338 – 339.
- [23] David A. Humphreys, Martin Hudlicka, and Irshaad Fatadin, "Calibration of Wideband Digital Real-time Oscilloscopes", Digest of Conference on Precision Electrical Measurements 2014, 24th August 2014, pp. 698 – 699.
- [24] David A Humphreys and Mira Naftaly, "Dynamic range improvement of THz spectroscopy", Digest of Conference on Precision Electrical Measurements 2014, 24th August 2014, pp. 704 – 705.
- [25] David Humphreys, Mira Naftaly, John Molloy, "Effect of Time-Delay Errors on THz Spectroscopy Dynamic Range" Digest of 39th Int. Conf. on Infrared, Millimeter, and THz Waves, September 2014, digest details not yet available.
- [26] David A. Humphreys, Martin Hudlicka, and Irshaad Fatadin, "Calibration of Wideband Digital Real-time Oscilloscopes", IEEE transactions on Instrumentation and Measurement, submitted in Aug. 2014.
- [27] Y. Deng, H. Füsler, and M. Bieler, "Absolute intensity measurements of cw GHz and THz radiation using electro-optic sampling", IEEE transactions on instrumentation and measurement, submitted in Aug. 2014.
- [28] M. Salhi, T. Kleine-Ostmann, G. Gentile, M. Spirito, and T. Schrader, "Planar Millimeter Wave Patch Antenna Arrays at 77 GHz and 94 GHz for Metrological Investigations", IEEE Transactions on Antennas and Propagation, submitted Sept. 2014.

IND16 Ultrafast



- [29] H. Füsler, M. Bieler, S. Ahmed, and F. Verbeyst, "Asynchronous electro-optic sampling of all-electronically generated ultrashort voltage pulses", Measurement, Science and Technology, submitted Sept. 2014.
- [30] M. Salhi, T. Kleine-Ostmann, and T. Schrader, "Antenna Characterization and Channel Measurements in the mm and Sub-mm Wave Region", Microwave Journal, submitted Oct. 2014.
- [31] David Humphreys, Mira Naftaly, John Molloy, "Dynamic range improvement of THz spectroscopy by digital signal processing and covariance analysis", to be submitted to IEEE Trans. Terahertz Science and Technology.
- [32] David Humphreys, Peter Harris, Faisal Mubarak, Dongsheng Zhao, Manuel Rodríguez-Higuero and Kari Ojasalo, "Do you have confidence in your RF waveforms?", to be submitted to Microwave Journal.
- [33] D. Allal, Y. Le Sage, A. Litwin, J.M. Lerat, "Cable effect correction for millimeter wave far-field radiation pattern measurements", to be submitted to Progress In Electromagnetics Research Letters.
- [34] M. Salhi, T. Kleine-Ostmann, and T. Schrader, "Broadband millimeter wave propagation measurements in indoor scenarios for future THz communication systems", to be submitted to IEEE Transactions on Antennas and Propagation.
- [35] M. Salhi, T. Granz, S. Rey, T. Kürner, T. Kleine-Ostmann, and T. Schrader, "Investigations on error vector magnitude for different modulation schemes in a 300 GHz transmission link", to be submitted to IEEE Transactions on Instrumentation and Measurement.